Spectral Discrimination of *Arundo donax L.* and *Phragmites australis* (Cav.) Grown Under Control and Accumulation of

Heavy Metal Conditions

A research report submitted to the Faculty of Science, University of the Witwatersrand, Johannesburg, in partial fulfilment of the requirements for the degree of Master of Science (Geographical Information Systems and Remote Sensing) at the School of Geography, Archaeology & Environmental Studies

Luphumlo Masiza (218031675)

Supervisor:
Prof Elhadi Block

September 2024

DECLARATION

I, Luphumlo Masiza, declare that this research report is my own unaided work. It is being submitted to the Degree of Master of Science in Geographical Information Systems and Remote Sensing to the University of the Witwatersrand, Johannesburg. It has not been submitted before for any degree or examination at any other University.

....

Signature of candidate

September .... **day of** ....03.......... **20**....24.................. **in** ... Buhlepark ....

Abstract

An approximate 50% decline in wetland loss worldwide has been estimated since the end of the 19th century (Kumari *et al.*, 2020). The escalating contamination of wetlands with heavy metals further poses significant threats to wetlands. As much as wetland plants may uptake heavy metals to aid in heavy metal reduction in the environment, contamination may have an impact on their physiological and biochemical properties. Impact in these properties may influence the spectral signature of the species. This study aims to spectrally discriminate between *Arundo donax L.* and *Phragmites australis* (Cav.) species under control and heavy metal conditions. The specific objectives are: (i) To discriminate between *A. donax* and *P. australis* species, both under control conditions and subjected to heavy metal treatment using field spectral measurements. (ii) Evaluate the discriminatory potential of resampled HyMap, WorldView-2 and WorldView-3, and Sentinel 2 data for distinguishing *A. donax* and *P. australis* under control and treatment conditions. (iii) To analyse the shift in the REP of *A. donax* and *P. australis* under both control and copper + acid treatment conditions. To do this, a glasshouse experiment with the two species where half of the tubs were exposed to copper and acid treatment (which mimic an acid mine drainage) and others left as controls was setup. Field spectroradiometer was used to take spectral reflectance measurements and features obtained from GGRF were used to discriminate the species using RF technique. Hyperspectral data was resampled to the different multispectral and hyperspectral sensors. Moreover, the concentration of copper in all the tubs were measured. There was no significant difference in the spectral reflectance of *A. donax* under control and treatment conditions. There is also no significant difference in the spectral reflectance when discriminating *P. australis* under control and treatment conditions. However, there is a slight significance when discriminating the two species when they are both under control. A significant difference in the spectral reflectance was obtained when discriminating the two species when exposed to the treatment. Random Forest classification showed an improved discrimination accuracy of 83.5% post-treatment, compared to 76.1% under control conditions. This shows discrimination was more effective after treatment, emphasizing the impact of environmental stressors on spectral responses. Resampling of hyperspectral data, especially using HyMap and WorldView-3, showed promise for discriminating between the species. The red edge position analysis indicated a slight stress-induced shifts of 2nm in *P. australis* (719 to 717 nm), while *A. donax* remained stable (719nm), suggesting resilience. It can be concluded that the species were better discriminated after the treatment of copper and acid, compared to when they are under control conditions.

Key words: *Heavy metals, Spectral discrimination, Random Forest classification, red edge position and remote sensing.*

Dedication

I dedicate this research to myself… I am proud of you.

Acknowledgement

Thank you, God, for continuously keeping Your promises and restoring my strength through all the challenges I faced.

I would like to sincerely thank my supervisor, Prof. Elhadi Adam, for his invaluable guidance and support throughout my academic journey. Thank you for not only giving me academic advice but also offering valuable life lessons, which have prepared me for the future.

To my friends and family, thank you for keeping me grounded throughout this journey.

Table of Contents

List of figures

List of Tables

List of Equations

Abbreviations

AD_T	*Arundo donax L.*
AGB	Aboveground Biomass
AMD	Acid Mine Drainage
ANN	Artificial Neural Network
As	Arsenic.
ASD	Analytical Spectral Devices
CART	Classification and Regression Trees
Cd	Cadmium.
Cr	Chromium.
Cu	Copper.
CuSO4	Copper sulfate.
EMS	Electromagnetic spectrum
Fe	Iron
g/cm^3	Grams per cubic centimeter, a unit of density.
GHz	Gigahertz
GRRF	Guided Regularized Random Forest
Hg	Mercury.
HMs	Heavy Metals
ICP-AES	Inductively Coupled Plasma Atomic Emission Spectroscopy
LAI	Leaf Area Index
LFPI	Linear Four-Point Interpolation
MLC	Maximum Likelihood Classifier
Mo	Molybdenum.
Ni	Nickel.

NIR	Near-Infrared
Nm	nanometers
OA	Overall Accuracy
OOB	Out-of-Bag
PA	Producer's Accuracy
PA_T	*Phragmites australis (Cav.) Trin. ex Steud*.
Pb	Lead
REP	Red Edge Position
RF	Random Forest
RRF	Regularized Random Forest
RS	Remote Sensing
SPSS	Statistical Package for the Social Sciences
SWIR	Shortwave Infrared Radiation
UA	User's Accuracy
VIR	Visible, Infrared, and Shortwave Infrared
WHO	World Health Organization
Zn	Zinc
ZnSO4	Zinc sulfate.
Mm	micrometers

CHAPTER ONE: INTRODUCTION

1.1 General Introduction

Rapidly increasing anthropogenic activities and industrialisation result in the rise of heavy metal concentration in freshwater systems such as wetlands. Wetlands support biodiversity, water purification, flood regulation, and carbon storage (An and Verhoeven, 2019; Bhowmik, 2022). These ecosystems also provide habitats for numerous species and breeding grounds for migratory birds and aquatic organisms. Wetlands act as natural filters, trapping sediments, nutrients, and pollutants such as heavy metals (HMs) (Sharma *et al*., 2021). However, persistent pollution of wetlands with HMs has become a serious environmental concern that can impact on aquatic biodiversity and humans (Ali *et al*., 2013). Adeeyo *et al*. (2022) state that human pollution, developmental activities, and invasive plants grossly endanger Wetlands in South Africa. Further stating, approximately 47.89% of reported wetlands lack sufficient protection and are therefore susceptible to various threats. Since 1900, an estimated 50% of global wetland loss has occurred (Kumari *et al*., 2020). According to Department of Forestry, Fisheries and the Environment, out of South Africa's identified wetland ecosystem types, 48%, 12% and 5% are classified as extremely endangered, as endangered, and as vulnerable, respectively. This presents a significant challenge to the progress toward achieving sustainable development goals (SDGs).

Some of the most prevalent HMs found in wetlands and rivers, causing harmful conditions for both aquatic life and humans, include copper (Cu), arsenic (Ar), lead (Pb), chromium (Cr), cadmium (Cd), and mercury (Hg) (Hong *et al.*, 2020). The primary human activities that release HMs to the environment include industrial processes, agriculture, urban runoff, and mining, which lead to acid mine drainage (AMD). The latter persists due to its pivotal role in South Africa's economic landscape, primarily involving the extraction and refinement of various minerals (Heisie *et al.*, 2023). Consequently, this process generates substantial amounts of waste, directly contributing to the accumulations of HMs in the country.

Recently, environmental contamination by HMs has become an increasingly significant concern globally (Tchounwou *et al.*,2012), Countries like Bangladesh and Italy have faced challenges related to arsenic contamination in groundwater, while Bolivia, Hong Kong, and Berlin have encountered HM contamination (Cd, Pb, and Cu) in drinking water sources (Rai, 2008). HMs contaminated is particularly a problem in developing nations. With the issue of consuming water contaminated with HMs being significant, primarily due to rapid population growth and insufficient financial investments in establishing secure and hygienic water systems (Abeer *et al.*, 2020). Addo-Bediako (2021) evaluated pollution levels on the Spekboom River in South Africa and found the presence of elevated concentrations of eight elements in the sediment, indicating a decline in quality of sediment, with notably high levels of Cr and Ni in across all studied sites. It is stated that the high concentrations of the latter may indicate contamination stemming from various anthropogenic activities in the area (Addo-Bediako, 2021). This shows the necessity of remediation measures to restore HMs polluted environments.

Phytoremediation is a sustainable approach that involves using plants to extract HMs in the soil, consequently leading to their reduction on the environment (Prasad, 2021). Species such as *Phragmites australis* (Cav.)

Trin. Ex Steud. (common reed) and *Arundo donax* (giant reed) are commonly used in wetlands, whether natural or man-made, for phytoremediation purposes (Sarath *et al.*, 2020). The two species are fast-growing and have high biomass production (Lino *et al.*, 2023; Zhang and Ye, 2009; Danelli *et al.*, 2021), which make them effective candidates for this remediation method. *Phragmites australis* accumulate HMs in aboveground and belowground biomass (Milke *et al.*, 2020), making them suitable for phytoremediation. The species have been demonstrated to grow on HM contaminated water and concentrate toxic elements in their root systems without significantly affecting their growth and development (Castaldi *et al.*, 2017). However, metal-contaminated water and soil may often manifest in the decrease of the leaf pigments, growth inhibition and have an influence on the concentration level of nutrients, especially in high concentrations (Deventer and Cho, 2014).

Hyperspectral remote sensing (RS) measures the reflectance of light across a wide range of wavelengths, providing a comprehensive insight on the chemical characteristics of a species (Liu *et al.*, 2011). It allows reflectance measurement in a broad range of the electromagnetic spectrum (EMS) (Poças *et al.*, 2011). Hyperspectral RS, such as field spectroscopy, is widely used and may discriminate species, identify existing stress and diseases in plants (Helmi *et al.*, 2010). Clevers *et al.* (2003) indicate that hyperspectral remote sensing has been shown to detect HM stress since the sensor influences the spectral reflectance of leaves (Clevers *et al.*, 2003). Hyperspectral sensors have also demonstrated potential in predicting plant biochemical and physiological attributes (Hassani *et al.*, 2023). This is because minor alterations in vegetation status, driven by shifts in foliage biochemical composition, have been demonstrated to impact the reflectance of vegetation at particular wavelengths (Cho *et al.*, 2008). Hence, RS based hyperspectral data is a powerful tool that can be used to detect HM impact in wetlands vegetation. RS techniques also help with saving costs and time compared to traditional monitoring techniques of measuring the presence of HMs in water, soils, or plants, which may be expensive and time-consuming.

Different studies have used RS to classify *Phragmites australis* and *Arundo donax*. A study by Onojeghuo and Blackburn (2010) identified the best combination of features for accurately mapping reedbeds with *Phragmites australis*, looking at how resolution impacts classification accuracy. The above-mentioned study further looked at the difference in the performance of different machine learning algorithms in classification accuracy. Another study discriminated against *Phragmites australis* wetland plants in the coast of the Gulf of Mexico using pixel-based Support Vector Machines classification with high-resolution imagery (Samiappan *et al.*, 2016). An overall accuracy of 91% was achieved, demonstrating the effectiveness of incorporating features such as morphological attribute profiles for accurate mapping compared to region-based approaches. In a study by Fernandes *et al.* (2013), *A. donax* was successfully discriminated from adjacent vegetation including *Phragmites australis* using a field spectroradiometer and a hierarchical procedure. The highest spectral separability was achieved after trimming *Arundo donax*. L (giant reed_RAC).

1.2 Problem Statement

Wetlands are some of the most important ecosystems that store fresh water. They provide important ecological services and products such as food, wildlife habitats and they also manage erosion and floods (Tshapa *et al.*, 2021; US EPA, 2015). Additionally, they contribute significantly to climate change mitigation efforts and provide recreational opportunities for both locals and tourists (Musabyimana and Bazimenyera, 2023). However, the escalating human activities in industry and agriculture have led to an increase in HMs presence in wetlands and the environment in general. This contaminates the environment and can deteriorate wetland ecosystem, and may lead to the presence of HMs in food chains. Thus, impeding progress towards SDGs 6 and 15, which speak on protecting water-related ecosystems such as wetlands and protecting biodiversity, respectively. Moreover, the National Water Act 36 of 1998 also talks about the importance of protecting aquatic ecosystems (DWAF, 1998). This shows the importance of protecting these water systems, especially because water is a scarce in SA (Nhamo *et al.*, 2020).

Arundo. donax and *Phragmite australis* are essential wetland plants. These species play a major role in phytoremediation which uses plants to take up HMs from the soil and water (Yan *et al.*, 2020). P *australis* and *A. donax L.* show tolerance to trace elements and are employed in constructed wetlands as well as for the remediation of contaminated soil and sludge (Bonanno, 2013). They enhance the quality of water in wetlands and, consequently, improve the state of the environment. Therefore, it is important for these wetland plants to be monitored to determine how they are affected by HMs and how effective they are at absorbing them. Additionally, because of *P. australis* ability to absorb HMs, these species indicate a potential as an effective biomonitoring tool (Cicero-Fernández *et al.*, 2017). *P australis* and *A. donax L.* are very similar to one another, and discriminating between the two species may be difficult. For example, Fernandes *et al.* (2013) successfully differentiated *Arundo donax* from other species; however, they faced challenges in distinguishing phragmites, as only a few wavelengths set the two species apart. However, these species may react to pollution differently, which may aid in discriminating them better. Hence, potential discrimination under stress conditions should be explored.

RS, particularly through the use of field spectrometers, holds significant promise in the spectral discrimination of species. Traditional methods of species discrimination often rely on visual inspection or laborious field surveys, which can be time-consuming, expensive and subjective (Deventer and Cho *et al.*, 2014; Müllerová *et al.*, 2013). However, field spectrometers offer a rapid and objective means of capturing detailed spectral information from vegetation. By measuring the unique spectral signatures of different plant species, field spectrometers enable precise discrimination between species based on their biochemical and structural traits (Mirzaei *et al.*, 2019; Pandey *et al.*, 2022). When vegetation is exposed to stressors such as pollutants, its reflectance properties can change in response ((Wang, Gao, and Zha, 2018). This alteration in reflectance is often indicative of physiological changes within the plant (Kior *et al.*, 2021). In turn, this may show when plants take up contaminants. Making RS ideal for monitoring and discriminating species whether they are healthy or under stressed conditions.

1.3 Aim and objectives

The aim of the study is to spectrally discriminate between *Arundo donax L.* and *Phragmites australis* (Cav.) species under control and heavy metal conditions.

The specific objectives are:

1. To discriminate between *A. donax* and *P. australis* species, both under control conditions and subjected to heavy metal treatment using field spectral measurements.
2. Evaluate the discriminatory potential of resampled HyMap, WorldView-2 and 3, and Sentinel 2 data for distinguishing *A. donax* and *P. australis* under control and treatment conditions.
3. To analyse the shift in the red edge position of *A. donax* and *P. australis* under both control and copper + acid treatment conditions.
4. To determine the statistical significant of copper concentration between A. donax and P. australis in both water and soil.

1.4 Research Outline

The research consists of five chapters, and the first chapter is the introduction, which introduces the topic and gives the problem statement, aims, and objectives. It is followed by Chapter two, which is the literature review. The literature review gives a brief introduction of the section, looks at wetlands' characteristics, their importance, and the existing threats to the wetlands. The chapter then dwells on heavy metals, looking at their sources, toxicity, and mechanism of HM uptake by plants (phytoremediation). This is followed by a section on monitoring HM uptake using RS, RS in spectral discrimination of plants and lastly, the REP. Chapter 3 Covers the research methodology. This includes the glasshouse experiment setup, measurements of spectral reflectance, analysis of spectral reflectance, analysis of spectral signature and feature importance selection using GGRF. This is then followed by an explanation of the random forest classifier, spectral resampling, how to extract the REP and copper concentration analysis. The results of the above methodology sections are illustrated and explained in Chapter 4 and discussed in Chapter 5. Lastly, the research concluded in Chapter 6.

CHAPTER TWO: LITERATURE REVIEW

2.1 Introduction

Arundo donax and *Phragmites australis* are important wetland plants providing ecosystem systems. They are used for erosion management because they have broad root systems and assist in preserving wetlands (Tshapa *et al.*, 2021). They help uptake HMs in both natural and constructed wetlands, which can change the spectral signature (Milke *et al.*, 2020; Khadidja *et al.*, 2019). This literature section will examine the wetlands and their characteristics, the importance of wetlands and threats to wetlands. It will further look at heavy metals, their sources, toxicity, and the mechanism of HM uptake by plants. The literature will also look at how remote sensing is used in monitoring HM uptake using wetland plants and spectral discrimination using remote sensing. The REP will also be explored.

2.2 Wetland Characteristics

According to Ramsar Convention (1971), wetlands are "*areas of marsh, fen, peatland or water, whether natural or artificial, permanent or temporary, with water that is static or flowing, fresh, brackish or salt, including areas of marine water the depth of which at low tide does not exceed six metres*". They occupy approximately 5–10% of the Earth's terrestrial surface (Kumari *et al.*, 2020). They help uptake heavy metals in both natural and constructed wetlands, which can change their spectral signature (Milke *et al.*, 2020; Khadidja *et al.*, 2019). This literature section will examine the wetlands and their characteristics, their different classes, the importance of wetlands and threats to wetlands. It will further look at heavy metals, their sources, toxicity, and the mechanism of HM uptake by plants. The section will also look at remote sensing technology, how the spectral signature of plants changes when exposed to plants and spectral discrimination using remote sensing.

2.3 Importance of Wetlands

Wetlands have an indispensable function in protecting ecosystem diversity, regulating climate change, supporting the well-being of the human population, and maintaining the global water cycle (Xu *et al.*, 2019). Some people around the world depend on wetland ecosystems to sustain their lives through its services. They provide both direct and indirect services such as wood, food, fibre, flood control, carbon sinks, and water recharge (Li *et al.*, 2014; Pan *et al.*, 2020; Chaudhary *et al.*, 2018). Wetlands also provide fresh water, help with water purification, and are a habitat for migratory birds (Dar *et al.*, 2020). They control floods by retaining water and storing nutrients and sediments moved by stormwater to avoid pollution in rivers and lakes. According to Aryal *et al.* (2021), more than 17% of Nepal's overall population relies on wetlands for essential livelihood services. At the same time, Isimangaliso wetlands in Kwazulu-Natal, South Africa, provide local community members with valuable ecosystem services (Orimoloye *et al.*, 2020). Moreover, wetlands contribute to the economy of a particular area by fostering recreational activities and serving as attractive destinations for tourists. Wetlands may effectively remove dissolved or colloidal metals from polluted groundwater (Moreau *et al.*, 2013). As a result, they are primarily used to reduce environmental contamination in mining zones. Studies demonstrate that natural and manmade wetlands are particularly employed to eliminate toxins from a range of wastes.

Furthermore, wetlands have been shown to have the ability to reduce or lessen pollution coming from agricultural regions and urban sewage (Bateganya *et al.*, 2015). Schulz and Peall (2000) looked at the effectiveness of a constructed wetland in taking up pesticide pollution in South Africa and found that the wetland effectively retains runoff-related agricultural pollutants. Wetlands use different chemical and bacterial processes to efficiently remove AMD in water, vegetation, and in the soil (Sheoran, 2006). In constructed wetlands, Sheoran (2006) states that pollutants in AMD are reduced through bioremediation and adsorption.

2.4 Threats to Wetlands

Regardless of all the direct and indirect services wetlands provide, they are still distracted and under a lot of threat. According to Kumari *et al.* (2020) An approximate 50% decline in wetland loss worldwide has been estimated since the end of the 19th century. This can be attributed to the increased anthropogenic activities, population, and climate change (Orimoloye *et al.*, 2020; Dar *et al.*, 2020; Adeeyo *et al.*, 2022). Rebelo *et al.* (2009) also state that wetlands are among the most threatened ecosystems from urbanisation and agricultural activities. This is because these activities result in habitat destruction and altercation (Blankenberg *et al.*, 2020). In South Africa, urbanisation has been seen as an issue since it leads to the establishment of unauthorized informal settlements, which consequently lead to high pollution of wetlands and other aquatic ecosystems (Adeeyo *et al.*, 2022). This is supported by Harmse and Le Grange (1994) who indicates that, in urban areas around Johannesburg, temporary wetlands show heightened concentrations of litter and nutrients attributed to increased human activities. This poses a problem because wetlands such as freshwater swamps are susceptible to the effects of predicted climate change (Shahi, 2020). With the key climate change effects of expected lower average rainfall, increased rainfall changes and drier seasons, and increased temperatures (Shahi, 2020).

Mining activities are also major wetland polluters around South Africa, as well as other countries. According to Ruppen *et al.* (2021), Mine tailings and deserted mines have a lasting impact on water resources well beyond the duration of a mine, primarily through the occurrence of AMD. AMD is a result of the reaction of oxygen and water with sulphide minerals, commonly in the form of pyrite, leading to the generation of acidic wastewater that is low in pH and HM (Wibowo *et al.*, 2022). For decades, AMD has been caused by seepage from tailings impoundments and water runoff from the surface from contaminated mine residue dumps (Sheoran, 2066). Byrne *et al.* (2013) provided evidence of neutral mine drainage impacts on macroinvertebrate communities. While another research found that freshwater at coal extraction areas is contaminated with Fe, Mn, Al, Ca, that damage the ecosystem and affect human life (Wibowo *et al.*, 2022). According to Riato *et al.* (2018), AMD is the predominant stressor in wetlands in South Africa's Mpumalanga Highveld region. In this area, coal mines use these wetlands to store contaminated water, directly releasing AMD into them. However, it is highlighted that planting certain plants can help clean up AMD pollutants in water (Mang and Ntushelo, 2019).

2.5 Wetland Vegetation Species

Wetland vegetation are plant species that are adapted to grow in water or periodically water saturated soil (EPA, 2023). There are a variety of wetland vegetation species with about 45 families identified worldwide of which some of them include Poaceae (Grass), Fabaceae, Brassicaceae, Cyperaceae, and Euphobiaceae (Newete and Byrne, 2016). In South Africa, Cyperaceae family is mostly found in warm parts of the country, e.g Kwa-Zulu Natal and the Kalahari (Gordon-Gray, 2009), and the grasses are distributed all around South Africa but mostly found in Kwazulu-Natal, Eastern Cape, and Free State (Sylvester, 2020; Sutton *et al.*, 2021). According to Hodkinson (2018), grasses are among the most important species due to the services and the products they offer. For example, sorghum is basic staple food, especially in Africa. The Poaceae family is inclusive of P australis and A donax which are widely distributed in SA.

Arundo donax L. is also distributed and invasive in countries such as Mexico, Australia, and some south parts of the United States (Canavan *et al.*, 2017). *A donax*, is indigenous to the Mediterranean region and has historically undergone cultivation for diverse purposes (Guarino *et al.*, 2020). Arundo is a perennial herbaceous rhizomatous plant which exhibits robust stems that attain heights ranging from 6 to 10 meters. While it does produce seeds, its primary mode of reproduction is via rhizomes. Because of its resilience and adaptability, *Arundo donax* has become established in various countries (Tshapa *et al.*, 2021; Canavan *et al.*, 2017). It was intentionally introduced in the country for various purposes, that include erosion management. However, it has become very invasive in SA (Canavan *et al.*, 2017). Nonetheless, Lino *et al.* (2023), state that it has limited threat because it does not reproduce sexually, facilitating the management of its spread. Canavan *et al.* (2017) also argues, stating that, its adaptability to different soil and weather conditions makes it competitive. In SA, *A. donax* has been shown to take over native species whilst it consequently put a threat to water security (Goolsby *et al.*, 2023; Canavan, 2016). Hence, it is also characterized as part of the most problematic invasive species in SA.

*Phragmites australis*is a globally distributed grass species with a wide native range encompassing temperate and subtropical regions in both hemispheres (Canavan *et al.*, 2019). It is native to SA and highly clustered in the Western Cape and Free State (Malapane, 2021). It is characterized by tall culms that have heights from 2 to 6 meters, have feathery flower heads and distinctive fluffy seed heads. They have high genetic diversity and can rapidly propagate through both seeds and rhizomes (Lambertini *et al.*, 2008; Kettenring *et al.*, 2015). According to Milke *et al.* (2021), *Phragmites australis* adapt to different soil and climate condition. This includes varying pH levels, salinity, and fertility. Despite their ecological importance in wetland ecosystems, common reed has the potential to become invasive, posing a threat to local biodiversity. They are present in the tropical Africa's forest, extending from Senegal to the east to Eritrea, and further south from Ethiopia and Eritrea to Mozambique, South Africa, and Swaziland (Milke *et al.*, 2021).

2.5 Heavy Metals

HMs are elements which have high density, typically higher than 5 g/cm^3, and have a potential of being toxic, making them a significant concern for human health and the environment (Duffus, 2002; Ali & Khan, 2018). Types of HMs include copper (Cu), zinc (Zn), mercury (Hg), lead (Pb), nickel (Ni), cadmium (Cd), chromium (Cr), and metalloids like arsenic (As). Some HMs are vital for organisms in small quantities but toxic in high concentrations. Such metals include zinc, copper, and nickel.

HMs such as Fe, Cu, Mo, and Zn function as cofactors and activators of several enzyme processes on plants and play an important part in enzyme/substrate metal complex formation. Amongst others, the most toxic HMs are lead, copper, cadmium, antimony, and thallium; which are prevalent in industrial processes (Mitra *et al.*, 2022). Metalloids, like thallium and arsenic, exhibit toxic properties by forming covalent bonds. This leads to the creation of lipophilic ions and compounds and can induce toxicity when binding to non-metallic elements in cellular macromolecules (Briffa *et al.*, 2020). Wetlands are often exposed to contamination high in HMs. Such pose a significant challenge as they are widespread and challenging to manage due to their ability to undergo structural changes, their ability to accumulate readily, and remain in the environment for extended periods (Yui *et al.*, 2021). They are also very hazardous and can pose a long-term ecological damage. These pollutants accumulate in the sediments via sedimentation and precipitation (Wang *et al.*, 2019). Thus, making the bottom of wetlands sinks for HMs, causing permanent potential harm (Yui *et al.*, 2021).

2.5.1 Sources of Heavy Metals

HMs have existed on Earth since its inception, undergoing continuous biogeochemical cycles (Masindi, 2018; Elnabi *et al.*, 2023). They are found all around Earth and are essential for survival, but their accumulation in organisms can be dangerous. Soil formation cause an increase in metal levels due to the weathering of bedrock, which contains a slightly higher concentration of HMs (Zaynab *et al.*, 2022). For example, carbonate rocks and silicate parent rocks contain trace metal contents (Wen *et al.*, 2020). A significant contribution to heavy metal pollution has also been reported from volcanic eruptions. (Nriagu, 1989). Although naturally occurring, human activities such as industrial processes, mining and agriculture can release them into the environment, polluting air, water, and soil. (Asrari, 2014).

2.5.2 Toxicity of HMs

The contamination of soil, air and water by HMs is a global environmental problem affecting millions of people around the world (Balali-Mood *et al.*, 2021). The impact of HMs on plants varies based on the plant type, particular metal, its concentration, chemical structure, soil makeup, and pH level. When metal concentrations surpass optimal levels within plants, they cannot be broken down, resulting in both direct and indirect adverse effects on the plants. The generation of free radicals in plant cells is one of the direct toxic effects of high HMs concentrations (Goyal *et al.*, 2020). This leads to oxidative stress and cell impairment as a result of different reactions (Goyal *et al.*, 2020). Indirect toxicity is caused by substituting essential nutrients at plant cation exchangers (Asati *et al.*, 2015).

Chlorosis and stunted growth are common in HM contaminated environments, indicating a disruption in photosynthetic pigment biosynthesis (Kumar and Aery, 2016). This interferes with plastid development, photosynthetic performance, and overall metabolism. (Kumar and Aery, 2016). Depending on the specific metal, the effects of HM toxicity on vegetation growth and development vary. Even at very low concentrations, metals such as Pb, Cd, Hg and As, are not vital in vegetation development. A series of experiments to investigate the effects of HMs (Pb, Cu, Zn) on Salvia species were carried out under greenhouse conditions. The plants were grown in pots with regular soil conditions, and stress was induced by introducing solutions containing various levels of HMs (Atanassova and Zapryanova, 2009). The plant height was highly affected by CuSO4 solutions, followed by solution containing ZnSO4 (Atanassova and Zapryanova, 2009). This contamination resulted in a decline in both tiller and panicle formation. According to Asati *et al.* (2016), the majority of the decline in growth indicators of vegetation cultivated in contaminated soils is as a result of decreased photosynthetic activity, plant mineral uptake, and a decrease in the activity of specific enzymes. This is supported by Rehman *et al.* (2021) who states that the development of plant organs and photosynthesis are affected by HMs.

The pollution of plants by HMs can have wider ecological consequences as it influences the food chain. Herbivores ingest plants contaminated with substantial quantities of HMs, which can accumulate in higher trophic levels, potentially impacting the environment and humans (Asati *et al.*, 2016). HMs like Cd and Hg are not essential for the human body's normal functioning and can be harmful, even in small amounts. According to Sodhi *et al.* (2022) and Shukla *et al.* (2022), the accumulation of metals in the body can interfere with its normal functioning, potentially resulting in health issues such as respiratory difficulties. Moreover, Cd in human bodies can impact adipose tissues and cause various health conditions such as obesity and hypertension (Tinkov *et al.*, 2017; Swayze *et al.*, 2021). According to Balali-Mood *et al.* (2021), exposure to Hg may result in peripheral nerve damage. Even when present in low concentrations, HMs have the potential to harm various organs, including the lungs and liver, and are also associated with disorders such as Alzheimer's (Zamora-Ledezma *et al.*, 2021; Elnabi *et al.*, 2023). According to Wang *et al.* (2019), common HMs found in wetlands include Pb, Cd, Hg, Zn, Cu, Cr, and Ni. Thus, their toxic effects will be discussed further below.

1.1.1.1 Cadmium

Cadmium soil and water contamination originates from both natural and human-driven sources and natural sources include bedrocks (Tran and Popova, 2013). In the aquatic environment, cadmium pollution arises from absorption, and industrial waste discharge, (Mitra *et al.*, 2022). Other sources encompass activities such as copper and nickel smelting and refining, burning of natural substances for fuel, and electronic waste recycling (Genchi *et al.*, 2020). In industrial settings, Cd poses risks through inhalation and ingestion, leading to acute and chronic intoxications. Studies indicate that the presence of Cd plays a significant part in polluting agricultural soil (Rani *et al.*, 2013). Its presence in plants result in growth inhibition and abnormalities in the overall development of various plant species (Tran and Popova, 2013). For instance, research by Vijayaragavan *et al.* (2011) demonstrated that cadmium reduces water adsorption, which is crucial for seed embryo development. Cd is considered a highly impactful pollutant because it is very toxic, and it has the ability to be easily dissolve in water.

1.1.1.2 Mercury

Although mercury comes from natural sources, it is highly produced by anthropogenic activities, and it is stated that the levels of mercury have tripled since industrialisation (Yang *et al.*, 2020). When mercury settles on aquatic floor, it becomes highly poisonous methylmercury (Gworek *et al.*, 2020). Mercury pollution in soil can hinder crop growth or cause plant mortality, ultimately impacting human health through the process of bioaccumulation (Qu *et al.*, 2019). To humans, exposure to mercury lead to nervous system related complication and other effects such as lung problems (WHO, 2021).

1.1.1.3 Chromium

While chromium is essential in minimal quantities for plants and animals, elevated concentrations pose a significant environmental contaminant. The adverse effects of chromium on plants amongst others include delayed seed germination, root damage resulting in reduced root growth, reduced biomass and plant size, leaf discolouration, inhibited nutrient uptake, necrosis, reduced grain yield and ultimately plant death (Srivastava *et al*., 2021; Sharma *et al*., 2020; Diaconu *et al*., 2020). High exposure to chromium in humans may affect the skin, lungs, kidneys, and liver (Ao *et al.*, 2022). Chromium is also cancerous to humans (Mitra *et al.*, 2022; Tchounwou *et al.*, 2012).

1.1.1.4 Zinc

The level of toxicity experienced is greatly dependent on both the manner and amount of exposure. Zinc, primarily originating from smelting and mining activities (Mitra *et al.*, 2022) has adverse impacts. Elevated concentrations of zinc in soil can lead to various changes in the plant, including diminished growth, lowered rates of photosynthesis and respiration, and change in the balance of minerals (Kaur and Garg, 2021; Balafrej *et al.*, 2020). Among the various physiological responses exhibited by plants to zinc toxicity, reduced germination vigor and biomass are particularly noticeable, ultimately resulting in decreased crop yield and diminished product quality (Kaur and Garg, 2021).

1.1.1.5 Nickel

Nickel serves as a prevalent industrial contaminant, often present in wastewater from industrial zones and landfills (Tognacchini *et al.,* 2020). Typically existing in either the Ni (0) or Ni (II) state due to their stability in water, this metal has been shown to impede cell division and elongation in certain plant species (Lešková *et al.*, 2020). In humans, nickel toxicity has gained recognition due to its association with cancer (Yusuf *et al.*, 2010). Research by Genchi *et al.* (2020) indicates that nickel exposure can lead to lung fibrosis, kidney, and cardiovascular ailments, and affect the respiratory system.

1.1.1.6 Copper

While Cu is crucial for humans and plants in smaller quantities, its detrimental effects become apparent when present in excess. In plants, it is essential for physiological processes, including the synthesis of chlorophyll. (Mitra *et al.*, 2022). According to Kumar *et al.* (2021) and Stern (2010), lack of Cu results in severe conditions such as anaemia and neutropenia. In contrast, high levels of Cu can lead to disorders in the liver and Alzheimer's disease and may also contribute to nervous breakdowns. In situations where copper concentrations are elevated, redox cycling might result in the release of free ionic copper. This could generate hydroxyl radicals, causing oxidative harm, or displace vital metal cofactors from metalloenzymes (Stern, 2010). An excess accumulation in plants has the potential to disrupt membrane integrity, reduce photosynthesis, and modify enzyme activity, leading to growth inhibition and other harmful effects in plants (Mir *et al.*, 2021).

2.5.3 Mechanism of heavy metals uptake (Phytoremediation)

Although metals can have harmful effects on a lot of vegetation, some of them have evolved mechanisms that help them withstand the presence of HMs and their toxicity (Dipu *et al.*, 2012). These mechanisms give plants the ability to accumulate and tolerate excess HMs that would have been toxic to other species (Dipu *et al.*, 2012). However, the ability of vegetation to take up HMs is determined by the specific species and the type and quantity of pollutants present. For example, Yang and Ye (2009), state that duck weed, and water hyacinth are great at accumulating of Cd and Cu. The ability of plants to take up HMs also depends on several environmental conditions, like the pH of the environment, temperature, and how saline the water is (Rezania *et al.*, 2019; Yang and Ye, 2009). Factors such as the grain size the physical, chemical, and biological conditions of the soil, fertility, and other ions' presence also control metal uptake (Yang and Ye, 2009). These plants uptake metals through a process called phytoremediation.

Plants have the capability to function as hyperaccumulators, accumulators and excluders. Hyperccumulators are able to gather metals in their above-ground parts, achieving concentrations notably higher than those present in their surroundings (Mganga *et al.,* 2011). They mainly use roots to uptake heavy metals, compared to absorbing using shoots (Pandita and Pamuru, 2022). And consequently, majorly accumulate them in the upper biomass of the plant (Pandita and Pamuru, 2022). However, certain plants exhibit the most significant accumulation of HM in the underground roots or stems. According to Yang and Ye (2009), numerous wetland plants exhibit elevated levels of metals in their roots compared to their shoots.

These plants accumulate heavy metals without negatively affecting plant growth (Yang and Ye, 2009). For example, Qian *et al.* (1999) state that water zinnia and smartweed accumulated One hundred forty-eight milligrams per kilogram of Cd and almost one hundred milligrams per kilogram, respectively, in their foliar without experiencing adverse effects. Khan *et al.* (2021) also found that *Euphorbia marginata* and *Cosmos bipinnatu* had no adverse effects after being grown on soil contaminated with 100 milligrams per kilogram of Cd. Many wetland plants are primarily HMs accumulators and have natural abilities to absorb, store, break down both organic and inorganic substances (Chatterjee *et al.*, 2010). These plants are typically metal-tolerant, fast-growing, and have a high biomass. (Zhang and Ye, 2009). Metal accumulators are distinguished by their rapid transfer of metals to the shoots and their notable capacity to breakdown and store HM in their foliar (Gunarathne *et al.*, 2018).

Plants take up HM in the exact mechanism they take up nutrients hence nutrient uptake is vital in phytoremediation. Keeran *et al.* (2021) found that plants capable of accumulating metals have developed mechanisms to tolerate the presence of these metals. This process involves the upregulation of specific proteins responsible for transporting and binding metals within the plant, including phytochelatins, metallothioneins, and other similar compounds, across various tissues. Through pH alterations, chelating agents produced by plant roots trigger redox reactions, rendering metals soluble for uptake, even at low soil concentrations (Pandita and Pamuru, 2022). The process of converting metals into soluble ions, particularly HMs, is primarily aided by the presence of rhizosphere bacteria and fungi that are closely related with the roots of vegetation (Pandita and Pamuru, 2022). These microorganisms play an important part in facilitating the solubilization of metals, making them more readily available for uptake by plants. Furthermore, the uptake of metals by root cells is facilitated by P1 ATPases (Keeran *et al.*, 2019). Table 2.5.3.1 below gives an overview of how plant species absorb heavy metals.

Table 2.5.3.1: Brief overview of HM absorption by plants.

Root Absorption	With their extensive surface area, the roots of such plants uptake HMs from both soil and water (Ghori *et al.*, 2019; Kumar and Aery, 2016). Additionally, they have the ability to excrete compounds that enhance the availability and absorption of HMs (Ghori *et al.*, 2019).
Transportation	HMs are transported using the xylem and phloem, after taken up by roots (He *et al.*, 2023).
Accumulation	The HMs are stored in various parts of the plant, e.g. leaves (Ghori *et al.*, 2019). Some plants can take up excess HMs in their tissues without being physically impacted (Kumar and Aery, 2016; Rascio and Nvaran-Izzo, 2011; Yang and Ye, 2009).

Phytoremediation, employing various wetland plant species, has been extensively used across the globe. One such plant species is the water hyacinth which has effectively removed contaminants in all seasons (Churko *et al.*, 2023). Water hyacinth was used in a Ramsar wetland for HMs removal and successfully removed more than 79% of metals (Rai, 2019). Another study used the same species to investigate the Zn uptake from polluted Lake Tempe (Nasir *et al.*, 2022). Water hyacinth absorbed a total of 77.3 ppm after a month. Another study used Alfalfa (*Medicago sativa L.)* to remediate artificially contaminated soil and found the plant to be effect in taking up Cd and Pb on the soil (Morsy *et al.*, 2022). Hasan *et al.* (2021) looked at the potential of using *Xanthium strumarium L.* for taking up chromium in contaminated Dhaleshwari River. The results showed a promise in the plant being used for phytoremediation because of its high translocation. In their study, Yang and Shen (2019) investigated the efficacy of *Typha latifolia L*. in the uptake of Cd from contaminated wetland at a laboratory. Their results showed the plant's strong tolerance to different Cd concentrations, accompanied by significant accumulation of the metal in its roots. Other studies have looked at the potential of *P. australis* and *A. donax* in phytoremediation (Al-Homaidan *et al.,* 2020; Azizi *et al.,* 2020; Zhang *et al.*, 2021; Ferrario *et al.*, 2022). Even though Rai *et al.* (2021) looked at *Phragmites karka* and *Arundo donax*, to the author's knowledge, there is no study that has looked at the effectiveness of both *P. australis* and *A. donax.*

P. australis and *A. donax*, are particularly efficient in phytoextraction because of their extensive root systems, tolerance to HMs and ability to grow fast (Zhang and Ye, 2009); Zhang *et al.*, 2014). They can thrive in contaminated areas, contributing to the mitigation of HM contamination in wetlands by reducing the concentrations of pollutants in the soil and water. *P. australis* and *A. donax* are used in artificial wetlands to treat wastewater. However, in naturally disturbed wetland environments, these plants assist in the process of water succession and contribute to the improving of the wetland ecosystem (Tshapa *et al.*, 2021). Studies show that the two species have been widely used in phytoremediation. For example, a study found that over a 6-week period, *Phragmites australis* demonstrated substantial removal capabilities, removing 93% of cd, 95% of Pb, and 84% of Ni from the environment (Bello *et al.*, 2018). It was found that *Phragmites australis* shows promise as a phytoremediator for extracting nickel (Ni) and lead (Pb) from Lake Burullus (Eid *et al.*,2021). Further stating that harvesting the above-ground biomass at its peak value could effectively reduce pollution in the lake. In another study, the potential of phytoremediation of Arundo donax and its symbiosis with Trichoderma harzianum for heavy metal-contaminated soils was assessed (Cristaldi *et al.* 2020). Results indicated effective bioaccumulation of metals, with enhanced performance in the symbiotic association, particularly for Ni, Pb, and Hg. The suitability of both *A. donax* and mycorrhized *A. donax* with T. harzianum for phytoremediation processes was demonstrated.

The different techniques of phytoremediation used by different plants are explained below.

2.5.3.1 Phytoextraction

Phytoextraction involves using plants to take up contaminants from the environment. The plants then transport and store these contaminants in their aboveground parts, such as stems and leaves (Yan *et al.*, 2020). Consequently, this removes HMs from contaminated soils, water, or sediments when these plants are harvested (Shen *et al.*, 2022). To be effective in this role, plants chosen for phytoextraction should demonstrate the capacity to withstand accumulated trace metal concentrations and possess efficient translocation abilities, coupled with substantial biomass (Bora and Sarma, 2019). According to Danelli (2021), phytoextraction is affected by the level of HMs in the aboveground biomass and the yield of dry biomass above the ground.

2.5.3.2 Phytofiltration

Phytofiltration involves using different parts of plants, such as roots, shoots, or seedlings, to absorb HMs from wastewater. (Yan *et al.*, 2020). This technique is particularly efficient for remediating soil and water with elevated nutrient contamination, specifically nitrogen and phosphorus (Kafle *et al.*, 2022). The effectiveness of this technique is attributed to the dense and extensive root system and the large surface areas of the roots, of the selected vegetation (Nedjimi *et al.*, 2021).

2.5.3.3 Phytostabilisation

Phytostabilization involves employing plant species tolerant to HMs to immobilize HMs underground (Kafle at al., 2022) thereby decreasing their availability for uptake. This helps keep them away from the environment while consecutively preventing them from entering the food web (Yan *et al.*, 2020). This means that certain vegetation species have the ability to alter HMs from a toxic state and reduce their toxicity. They achieve this through various processes within the plant, such as adsorption and precipitation, as discussed by Shen *et al.* (2022).

2.5.3.4 Phytovolatilization

Phytovolatilization transforms HMs to less harmful volatile forms within the plant (Yan *et al.*, 2020). Subsequently, releasing them into the atmosphere through the process of plant transpiration, primarily occurring through the leaves (Yan *et al.*, 2020; Thakur and Kumar., 2024). The metals that have been used in this technique include Hg, As, Se and organic compounds (Bora and Sarma, 2019). Additionally, Kafle *et* *al.* (2022) outlines that, some compounds may undergo direct volatilization from stems and leaves, while others may volatilize as a result of interactions at the root-soil interface.

2.7 Monitoring HM Uptake of Wetland Plants using RS.

The effectiveness of phytoremediation is demonstrated by many studies as stated above; however, the effectiveness of the process has to be assessed. Traditional approaches, such as chemical analysis can be time-consuming, destructive, and complicated (Diarra *et al.*, 2022). Monitoring tree rings for analysing contamination can also be time-consuming (Burken *et al.*, 2011). Given that exposure to HMs changes the structure and foliar characteristics of plants, leading to changes in their spectral reflectance, RS emerges as a viable and efficient method for monitoring plants used in phytoremediation (Kumar *et al.*, 2022). Mondal *et al.* (2020) also states that vegetation indices such as the NDVI can be used to aid in monitoring contaminated areas. The REP (670-780) is a critical indicator of pollution, especially from HMs. Saha *et al.* (2022) states that the visible and REP (535-640 nm and 685-700 nm, respectively) are particularly sensitive to stress. While Zhou *et al.* (2018) states that stress-induced changes also lead to increased reflectance at around the 680 nm absorption point. This shows that the REP aids in revealing the status of contamination in the surrounding environment (Noomen *et al.*, 2015). Studies using RS have also revealed spectral changes in plants growing in metallic conditions, particularly focusing on shifts in the REP as a response to metal-induced stress (Horler *et al.*, 1983; Rock *et al.*, 1988).

HMs also alter other parts of the EMS, making it possible to RS to be used in monitoring. For example, HMs alter leaf reflectance characteristics by increasing the spectral signature in VIR, decreasing it in the NIR, and shifting the REP to shorter wavebands (Wang *et al.*, 2015). Moreover, under stress or metal exposure, chlorophyll content decreases, resulting in a shorter wavelength. When chlorophyll decrease due to stress, it leads to high reflectance between 530 nm and 670 nm (Roman and Ursu, 2016). Rathod *et al.* (2015) investigated the impact of HM exposure on barley leaves' spectral reflectance and found that arsenic specifically influenced the visible and infrared regions. The sensitivity of plant spectral reflectance to pollution suggests that reflectance characteristics can serve as indicators for pollution uptake. This implies that RS can be effectively employed for monitoring plants in polluted environments. The spectral range of 350-3500, fine spectral resolution and the high coverage of the EMS make it ideal for analysing vegetation when under stressed conditions. ASD field spectroradiometer has played a crucial role in quickly assessing various physiological and biochemical traits of maize leaves. Through hyperspectral reflectance, this instrument allows for the evaluation of traits such as chlorophyll content, nitrogen levels, and photosynthetic activity in maize leaves, enabling efficient and thorough phenotyping of the plants (Yendrek *et al.*, 2016). Field spectrometer data was also used in assessing the morphological changes of fruits when exposed to HMs (El *et al.*, 2020).

2.8 Remote Sensing in Spectral Discrimination of Vegetation

RS plays a pivotal role in the spectral discrimination of vegetations, offering valuable insights into vegetation characteristics and distribution patterns. RS uses a spectral library to help identify match observed spectral patterns with known signatures (USGS, 2024). This means every vegetation, soil, water, and other various materials have a unique spectral signature. This means different species can be discriminated from one another and healthy and unhealthy species can be discriminated. Fernandes *et al.* (2013) assessed the ability to distinguish the invasive *A. donax* from neighboring vegetation using a field spectroradiometer. The study used a hierarchical approach across various phenological stages and post-cutting scenarios of giant reed stands. The results demonstrated significant spectral separability for giant reed, particularly in stands regenerated after cutting. Iqbal *et al.* (2021) used a ground-based hyperspectral sensor to distinguish between invasive and native plant species in Punjab, Pakistan. Significant spectral differences were found among various species, with red-edge parameters showing the greatest discriminatory potential (85%). Prospere *et al.* (2014) discriminated wetland plant species using hyperspectral data and the RF classifier successfully discriminated the plant species and achieved over 90% and 84%. Another study spectrally distinguished nine common tea plant varieties amongst six natural plant species in India, employing in situ hyperspectral data alongside machine learning methodologies (Nidamanu, 2020). Results revealed successful separated on only six tea plant varieties, achieving accuracies between 75% and 80%. Many other studies discriminated plant species from each other using RS techniques (Manevski *et al.*, 2011; Zhao *et al.*, 2022). While other studies used resampled data. For example, Gasela *et al.* (2024), used nSight-2 hyperspectral data to discriminate wetland plants in South Africa. In this study, Partial Least Squares Discriminant Analysis, Random Forest, and Support Vector Machine were used to spectrally separate wetland plants. The results found Support Vector Machine to be effective (OA=93.2), compared to the other two techniques which achieved an OA between 80% and 85%.

2.9 Red Edge Position

The REP refers to a critical point in the spectral reflectance curve of vegetation, particularly the sharp increase between the red and near-infrared wavelengths (670-780nm) (Ali and Imran, 2020). This unique point is a result of the change in the absorption of chlorophyll in the red region and the scattering of light in the NIR region. REP serves as a critical measure of plant health and physiological condition because it is very responsive to alterations in chlorophyll content, leaf area index, and the overall structure of vegetation (Zarco-Tejada *et al.*, 2018; Ali *et al.*, 2022; Ali and Imran, 2020). Making it a valuable indicator for assessing plant health and physiological status (Sellami *et al.*, 2022; Delegido *et al.*, 2013). Recently, RS techniques have optimized the use of the REP to monitor and assess plant health. Filella and Peñuelas (1994) discussed the relevance of the REP as a point which shows plant health aspects like the chlorophyll present, biomass, and water content. Sun *et al.* (2023) demonstrated the use of the REP to improve leaf area index estimation, highlighting the importance of the REP in characterizing vegetation biophysical traits. Wu *et al.* (2019) also states that the REP is commonly used to read HM stress on plants. Additionally, Zhu *et al.* (2013) employed a hyperspectral derivative ratio within the REP to detect plant stress caused by gas leaks prior to the manifestation of visible symptoms.

The REP has been investigated in studies examining the impact of environmental stressors, such as copper and acid, on plant health. Horler *et al.* (1983) observed that HM-treated plants have lower chlorophyll levels than healthy plants, indicating a potential shift in the REP due to HM stress. A study by Iqbal *et al.* (2021) spectrally discriminated between native and invasive species and found that the REP was the most effective in discriminating between the species. Another study assessed the effects of HMs in plants exposed to mine contamination (Zhou *et al.*, 2018). Yet again, the REP was found to be sensitive and was able to detect the stress imposed. These findings indicate a link between heavy metal exposure and shifts in the REP, reflecting alterations in plant pigments and physiological status. Moreover, Mensens *et al.* (2017) demonstrated that morphological traits predicted changes in diatom density, photosynthetic efficiency, and fatty acid production in the presence of Cu, showing an association between copper-induced stress and shifts in the red edge position. These findings on studies show the importance of the REP as a sensitive indicator of environmental stress and its potential utility in monitoring plant health and stress responses.

CHAPTER THREE: METHODOLOGY

3.1 Glasshouse Experiment Setup

In a controlled experiment at the University of the Witwatersrand, Johannesburg, South Africa, rhizomes of *A. donax* (giant reed) and *P. australis* (common reed) were collected from Lake Florida in January 2018. These rhizomes were then planted in sand-filled rooting beds. After 21 days, individual rhizome cuttings, each with a single plant reaching around 12 cm in height, were selected, and transplanted into 26 tubs for each plant species, *A. donax* and *P. australis*. Gravel, sand, and topsoil were layered within each tub, and regular irrigation was maintained to keep water levels approximately 8 centimetres above the topsoil.

After a three-month acclimatization period and biomass growth in the experimental tubs, treatments were introduced. Thirteen of the tubs for each reed species underwent treatment, with the addition of 5mg/L of copper from a prepared stock solution containing cupric sulphate pentahydrate (CuSO4.5H2O) and nitric acid, adjusting the solution to a pH of 3-4. This was done to replicate the presence of copper contamination resulting from pollution in wetlands caused by acid mine drainage. The remaining half (13) of the tubs for each reed species served as control groups, without Cu + acid treatment. The experiment lasted for 3 months and after this duration, the leaves spectral reflectance from the surviving tubs were measured and the soil and water samples were given to the laboratory of Agricultural Research Council-Institute for Soil Climate and Water (ARC-ISCW, Pretoria) for copper analysis.

3.2 Measurements of Spectral Reflectance

The spectral characteristics of *Arundo donax and Phragmite australis* were analysed utilising the Field Spectrometer provided by Analytical Spectral Devices (ASD). Operating within the spectral range of 350 to 2,500 nanometres (nm) and a bandwidth of 3 nanometres, this spectroscopic instrument captures data across the visible and near-infrared regions. Allowing for effective substance identification and analysis due to distinct reflectance properties (Singh *et al.*, 2020). The instrument is equipped with a contact probe, which helps in taking spectral reflectance measurements while minimizing external interference. The contact probe facilitates calibration using a white reflectance panel and incorporates a dark panel for reflectance measurement. For each tub containing both *P. australis* and *A. donax*, 12 spectral reflectance measurements by taking three repeated measurements on four randomly selected leaves from each tub were conducted. This involved making a random selection of four leaves, taking three measurements on each chosen leaf, and averaging the results to represent each tub. This was done using the ASD leaf clipper, and the whole process was repeated for a total of 188 leaves. Subsequently, the collected spectra underwent preprocessing using ViewSpecPro 6.2 software, and the processed data were saved to obtain reflectance values at each nanometre interval.

3.3 Analysis of Spectral Signature

3.3.1 Feature Importance Selection using GGRF.

The dataset exhibited a high feature-to-sample ratio, leading to the common issue of multicollinearity, where some features may be highly correlated or redundant (Konietschke *et al.*, 2021). To mitigate this challenge, the Regularized Random Forest (RRF) and Guided Regularized Random Forest (GRRF) techniques for feature selection and model regularization were employed. RRF integrates regularization methods within the random forest framework to address multicollinearity and overfitting. This is achieved by placing constraints on certain features during the model construction process, effectively reducing the influence of less significant or correlated variables. GRRF builds upon RRF by incorporating additional techniques into the random forest algorithm to selectively choose important features. The approach follows the methodology outlined by Deng and Runger (2013) and Izquierdo-Verdiguier *et al.* (2017).

Given a dataset *X* which consists of *n* samples, each containing *p* features. X can be viewed as a matrix [xi, j] i∈1...n,j∈1...p associated with a labels vector Y seen as [yi]i∈1...nAs feature selection is of interest, X can also be represented as [X_1, X_2,X_3…,X_P], i.e., X_k denotes the vector of feature k. Now feature j's importance in RF is calculated as:

$$Importance_i = \frac{1}{no.trees} \sum_{v \in SXi} Gain(X_i, v) \text{ .... } 0.1$$

Where X is the training data set and $Gain(X_i, v)$ represents the gain in the Gini index at each node (v) based on each feature (xj). $no.trees$ is the total number of trees present. Using Random Forest (RF) as a feature selection method entails either setting a predetermined number of features to select (K) or defining a threshold based on feature importance. The integration of regularization effectively addresses and resolves those challenges.

The GRRF model uses the original feature importance scores derived from RF and defines the normalized importance score as:

$$Importance'_i = \frac{Importance_i}{max_{i=1}^{p} importance_i} \quad \text{...........} 0.2$$

Imp_i = importance score, obtained from RF (Equation 3.3.1) where 0≤ Imp_i ≥ 1.

The GRRF technique chooses the number of features by employing an individual regularization parameter for each feature. This parameter retains the gain (as in equation 1) obtained from the features chosen in earlier nodes and penalizes the gain associated with newly created features. Consequently, the GRRF feature importance is calculated as:

$$Gain_R(X_i, v) = \begin{cases} \lambda . Gain(X_i, v) & i \notin F \\ Gain(X_i, v) & i \in F \end{cases} \text{ ....} 0.3$$

F represents the set of features used for splitting in preceding nodeswhile αj denotes the regularization parameter assigned to each feature, determined by:

$$\alpha_j = (1 - \gamma) + \gamma \frac{importance_j}{max_{j=1,\dots,p}(importance_j)} \text{ ....} 0.4$$

Note that γ ∈ [0, 1] represents the weight of the normalized importance, and when γ = 0 the GRRF reduces to the RF method

3.3.2 Random Forest Classifier

Random Forest (RF) is a machine learning technique that enhances regression and classification (Breiman, 2001). Random Forest leverages the combination of multiple decision trees created through bagging and random feature selection to build an ensemble model that reduces variance, maintains low bias, and produces robust and accurate predictions by aggregating diverse but approximately unbiased models (Zhao *et al.*, 2022). This technique was selected due to its ability to yield high accuracy and the presence of a large sample size (Misra and Li, 2020). To conduct classification in RF model, 70% of the dataset is used for training the model, and its performance is tested on the remaining 30%. This technique creates multiple decision trees through bootstrap sampling and aggregation of predictions, jointly known as bagging (Mureriwa *et al.*, 2016). Each tree gets a vote, ultimately determining the most frequent class assigned to the input data. Bootstrapping ensures that each decision tree within the ensemble is distinct, collectively reducing overall variance and avoiding overfitting (Misra and Li, 2020). This approach ensured that the model was trained on a substantial portion of the data while preserving an independent subset (30%) for internal cross-validation to new, unseen data known as out-of-bag (OOB). This result in an error estimated known as the out-of-bag (OOB) error.

The OOB samples undergo classification by traversing down the tree's structure. This sequential process yields predictions for OOB samples based on the tree's structure. Subsequently, this procedure iterates through all trees (no. of trees=500) in the random forest, employing the OOB samples to generate predictions. The accumulation of these predictions involves aggregating votes generated by different trees for each OOB sample. This process is repeated for all trees in the random forest, generating predictions for OOB samples by different trees. Followed by aggregating the predictions by majoring voting. The aggregated OOB predictions are compared to the true classes of the OOB samples. The frequency of disagreement between the predicted and true classes is calculated, assessing how often these mismatches occurred across all OOB samples. This process gives the average disagreement, which give the OOB error estimate, indicating the classifier's accuracy without a need for a separate test set or cross-validation (Zakariah, 2014).

The RF classifier’s accuracy was evaluated using a confusion matrix to calculate the overall accuracy (OA), users’ accuracy (UA), and producer's accuracy (PA). The Overall Accuracy (OA) in a confusion matrix indicates the overall percentage of correctly classified instances, Producer's Accuracy (PA) evaluates how accurately a model can identify instances belonging to a particular class among all the actual instances of that class. On the other hand, the UA assesses the model's precision in accurately identifying instances of a particular class among all the instances classified as that class by the model.

3.4 Spectral Resampling

The spectral characteristics of *Arundo donax* and *Phragmites australis* species were resampled to align with selected spectral resolution of hyperspectral and multispectral sensors. The 350–2500 nm spectral range was resampled using the spectral resampling tool to match the spectral bands of the HyMap, WorldView-2, WorldView-3 and Sentinel 2 images. The main objective of resampling in this study was to determine if the multispectral satellite sensors and HyMap hyperspectral sensors would be able to discriminate between the species when under control conditions and treatment. Other benefits of resampling include that it facilitates meaningful comparisons, promoting consistency in spectral information across different RS platforms. Such standardization is vital for promoting efficiency and accessibility in RS studies that involve both hyperspectral and multispectral data. Resampling also enables the use of cost-effective and widely available multispectral imagery for use in discriminating species. For example, Sentinel 2 is freely available hence it was considered. On the other hand, WorldView data was chosen due to its high spatial and spectral resolutions, as noted by Tesfamichael *et al.* (2022), making it suitable for an effective comparison across various resolutions commonly used in multispectral RS systems. The resampled data was subsequently classified using the Random Forest technique upon selection of the important bands as described above. This process was executed within ENVI Classic 5.3, utilising an ASCII format file containing central wavelengths for each resampled spectrum.

3.5 Red Edge Position

The red edge position (REP) in vegetation spectra is affected by biochemical characteristics such as the amount of water in the leaves, the concentration of chlorophyll, and other constituents present in the plant (Fu *et al.*, 2020; Croft and Chen., 2018). Changes in these biochemical properties due to metal stress and other factors can cause shifts in the reflectance of vegetation in the REP (Fu *et al.*, 2020; Wu *et al.*, 2019). Monitoring changes in the REP gives valuable information about the physiological state and health of vegetation, making it a crucial indicator in RS and ecological studies. Hence the REP shift was determined before and after treatment of copper and acid. To do this, the REP from the data was extracted using the Linear four-point Interpolation (LFPI) technique. The LFP method uses four points; 680, 700, 740 and 780 under the assumption that the reflectance curve can be simplified to a linear trend at the red edge. This edge is usually located approximately halfway between the reflectance peak in the near-infrared (NIR) spectrum, which occurs around 780 nm, and the point of lowest reflectance corresponding to the absorption of chlorophyll, which is approximately at 670 nm. This is computed using two steps: Step 1 - Computing the reflectance value at the inflection point (R_{re}):

$$Rre = R780 + R670/2 \ldots\ldots\ldots\ldots 0.1$$

Where R is the reflectance and Rre is used in REP computation.

Step 2 - Computation of the REP:

$$REP = 700 + (740 - 700) * [Rre - R700/R740 - R700] \ldots\ldots\ldots 0.2$$

3.6 Copper Concentration Analysis

Copper concentrations in both soil and water were analysed for *A. donax* and *P. australis* plants in all tubs. Soil samples from each tub were air-dried for three days and then securely packed in labelled plastic bags, each containing 500g of soil. Simultaneously, to prepare water samples for analysis, there were collected in 500ml bottles and promptly refrigerated until their transfer to the laboratory. The analysis of copper was conducted at ARC-ISCW Laboratory, using inductively coupled plasma atomic emission spectroscopy (ICP-AES) for accurate and precise measurements of copper concentrations.

Following the receipt of the results, a comprehensive statistical analysis was conducted. The study employed the independent-samples t-test within the SPSS software to explore potential statistical variances in mean copper concentrations. The analysis focused on the copper means in the soil and water for each plant species, aiming to identify any statistical significance within the tubs containing the two plants. Additionally, the study analysed if there was a statistical significance in the mean copper concentration between the tubs of the two plant species in both water and soil. A 95% confidence interval for the mean was applied, corresponding to a significance value of $p < 0.05$.

CHAPTER FOUR: RESULTS

4.1 Statistical Analysis of Copper and Acid; and Species Spectral Characteristics.

Copper concentration in soil and water of the *A donax* and *P. australis* tubs were measured and analysed using the independent samples test. Based on the t-test results (p-value = 0.227), the mean concentration difference of copper (Cu) concentrations on the soil between the two groups (A donax and *P. australis*) is not significant. When looking at the copper concentration in water in the two tubs of the species, a p-value of 0.373 is obtained, which is bigger than the significance level of 0.05. This means there is no significant difference in means between the two groups. Additionally, the mean concentration of copper in *A. donax* and P australis tubs were analysed and compared in water and on the soil. The measured mean concentration of copper in the A. donax tub was 5.57 mg/kg in soil and 0.02 mg/kg in water. In *P. australis* tub, it was measured as 0.29mg/kg in water and 7.19 in the soil. Based on the t-test, p= <0.001, this means there is significant difference in the mean Cu concentrations between the two groups. The assumption of equal variances is violated. Sample size was measured using Cohen's d, which is a standardized measure of effect size that represents the difference between the means of two groups in terms of standard deviations. In this instance, Cohen's d indicates a large effect size and also suggests that the mean difference between the groups is more than two standard deviations.

Figure 4.1.1 and Figure 4.1.2 show the spectral signatures of *Arundo donax L.* (AD_C) and *Phragmites australis (Cav.) Trin. ex Steud.* (PA_C) in controlled conditions and post-treatment with copper and acid, respectively. This means that there is a variation in the reflectance of the two species when they are both under controlled conditions and when under treatment conditions. Under controlled conditions, effective discrimination in the two species is evident in the VIR, slightly in the NIR, shortwave NIR, and to some extent in the red edge. However, following treatment with copper and acid (Figure 4.1.2), the discrimination becomes more prominent, particularly in the NIR and SWIR regions. The spectral signature of *Phragmites australis* is higher across the whole spectrum. However, there is a change when the species are exposed to copper and acid treatment where phragmite australis is lower in the visible region.

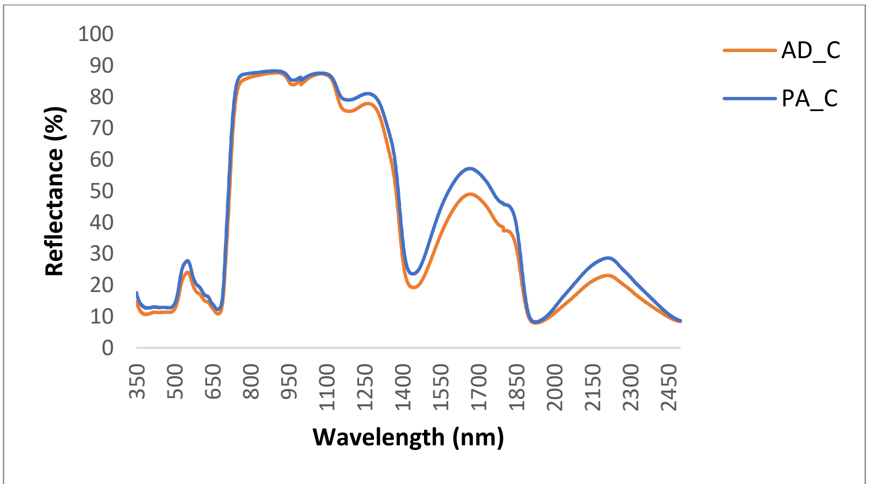

Figure 0.1 Hyperspectral reflectance of AD_C and PA_C under controlled conditions.

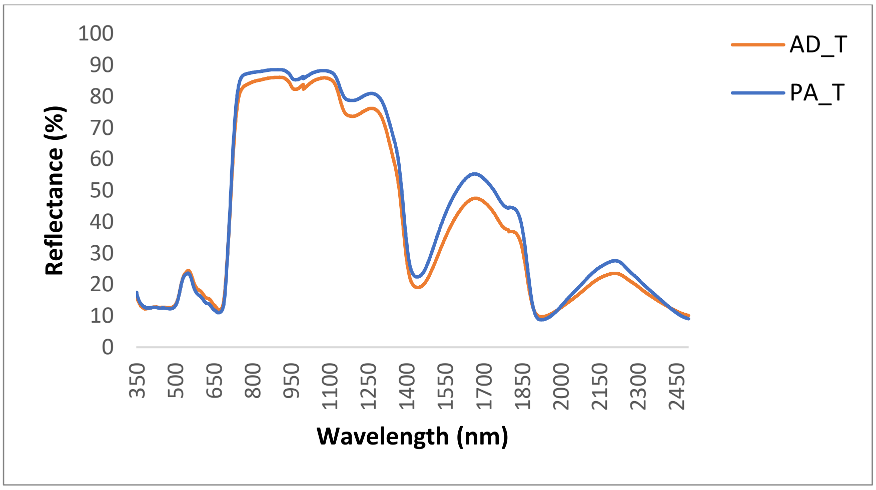

Figure 0.2 :Hyperspectral reflectance of AD_T and PA_T post treatment.

In Figures 4.1.3 and 4.1.4, the reflectance patterns of *A. donax and P. australis* are shown for both control conditions and after treatment. Effective discrimination between the *A. donax* control and treatment is observed, albeit to a limited extent, through the VIR, NIR, and SWIR. Conversely, effective discrimination between the control and treated conditions of *P. australis* (Figure 4.1.4) is demonstrated prominently in the VIR and SWIR regions.

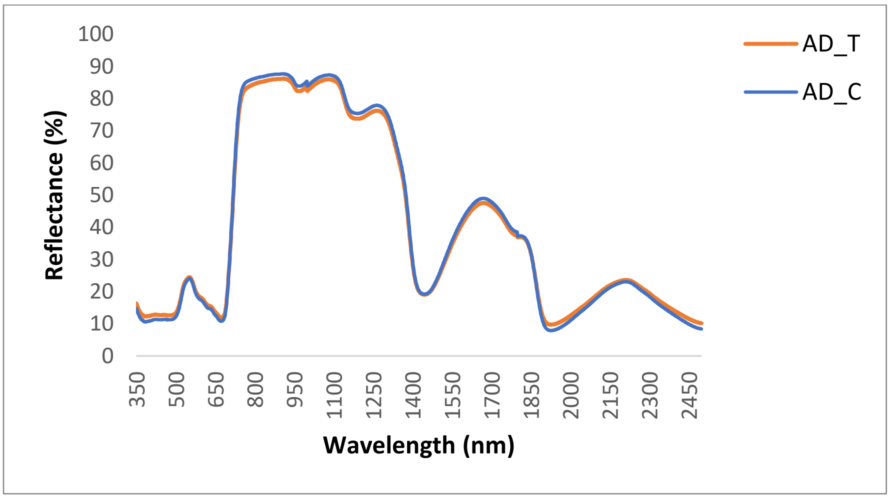

Figure 0.3 Hyperspectral reflectance of AD_T before and post treatment.

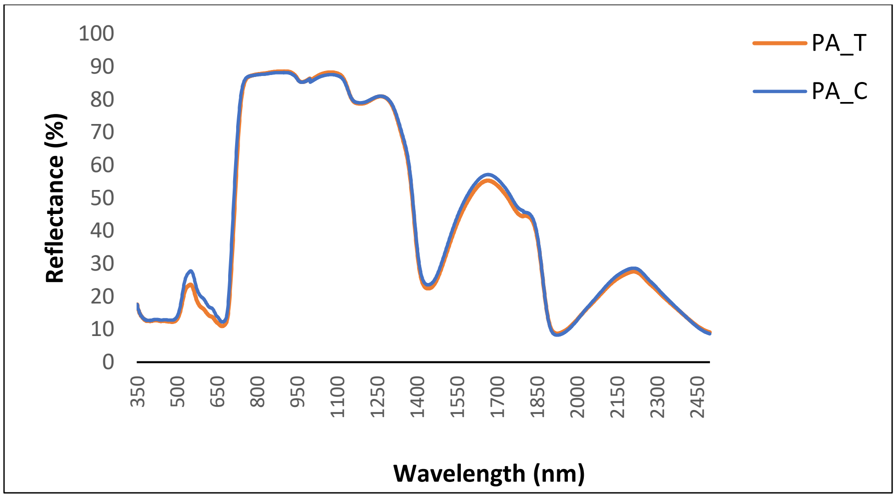

Figure 0.4 Hyperspectral reflectance of PA_T before and post treatment.

4.2 Feature Importance Selection Measurement

The RF technique effectively reduced correlation and redundancy, allowing for the selection of important wavelengths in discriminating the species from a pool of 2151 hyperspectral bands/features. Figure 4.2.1 illustrates the variations in selected important wavelengths for AD and PA species under control conditions and when subjected to copper and acid treatment. The most important wavelengths are characterized by a high Gini index value and when both the species are under control, the most important bands associated with clusters are found in the VIR, NIR and far SWIR of the electromagnetic spectrum.

Upon treatment of the species, the Gini index clusters are lower, and the most important wavelengths remain in the VIR region, and shift towards the REP and near shortwave-infrared spectrum. Figure 4.2.1C and D shows the variation in the importance wavelengths of *A. donax* and *P. australis* both under control and treatment. Most importance wavelengths of *A. donax* are seen across the whole spectrum and those of *P. australis* are seen on the VIR, NIR as well as the near SWIR regions.

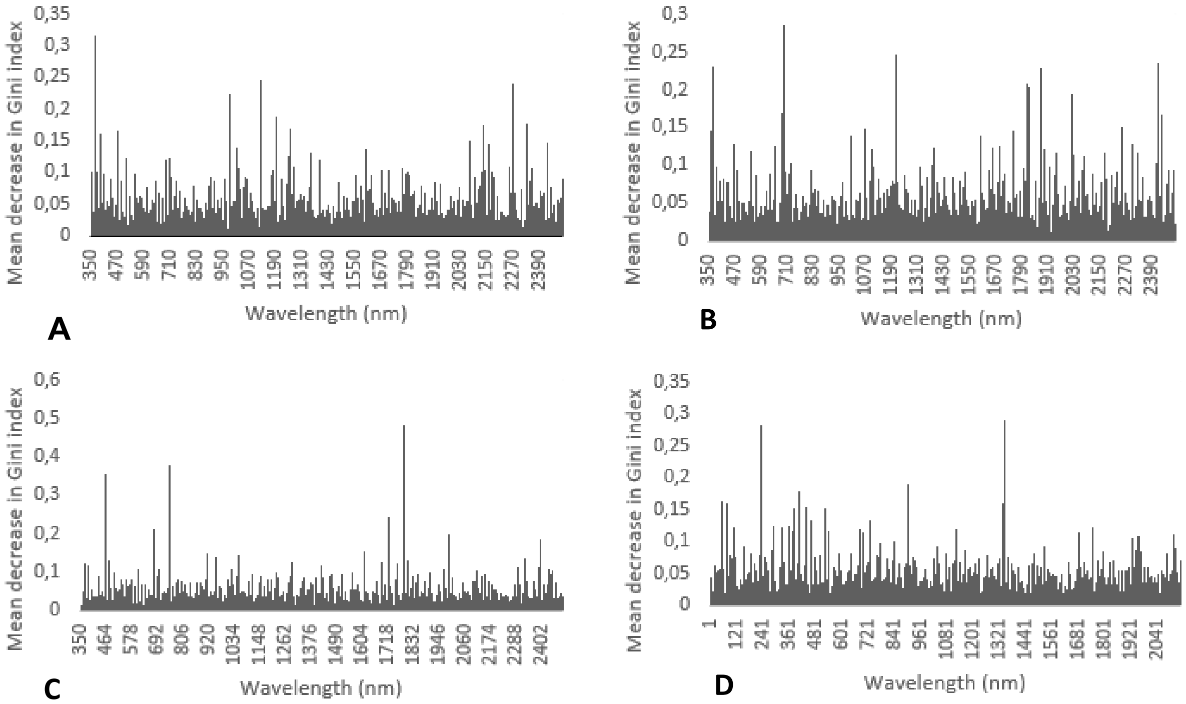

Figure 0.1 Selected wavelengths measured by ordinary RF using mean decrease in Gini Index for distinguishing between (A) AD_C and PA_C under controlled conditions, (B) AD_T and PA_T post treatment, (C) AD_T and AD_T post treatment. (D) PA_T and AD_T post treatment.

In Figure 4.2.2, the most crucial wavelengths are illustrated based on the GRRF selection using the importance bands identified by ordinary RF. For *A. donax* and *P. australis* species under control conditions, the selected importance wavelengths are 370, 981, 1125, 1192, 1607, 2072, 2271, and 2333. After treatment, these species exhibit different sets of importance wavelengths, namely 461, 747, 1722, 1791, 1995, and 2399. The selected importance wavelengths for A donax under control and treatment are 366, 370, 698,1073, 1211, 1819, 1880, 2021, 2172, and 2420. On the other hand, *P. australis* has the importance bands as 581, 757, 1255, 1693, and 1726 when under control and after treatment with copper and acid.

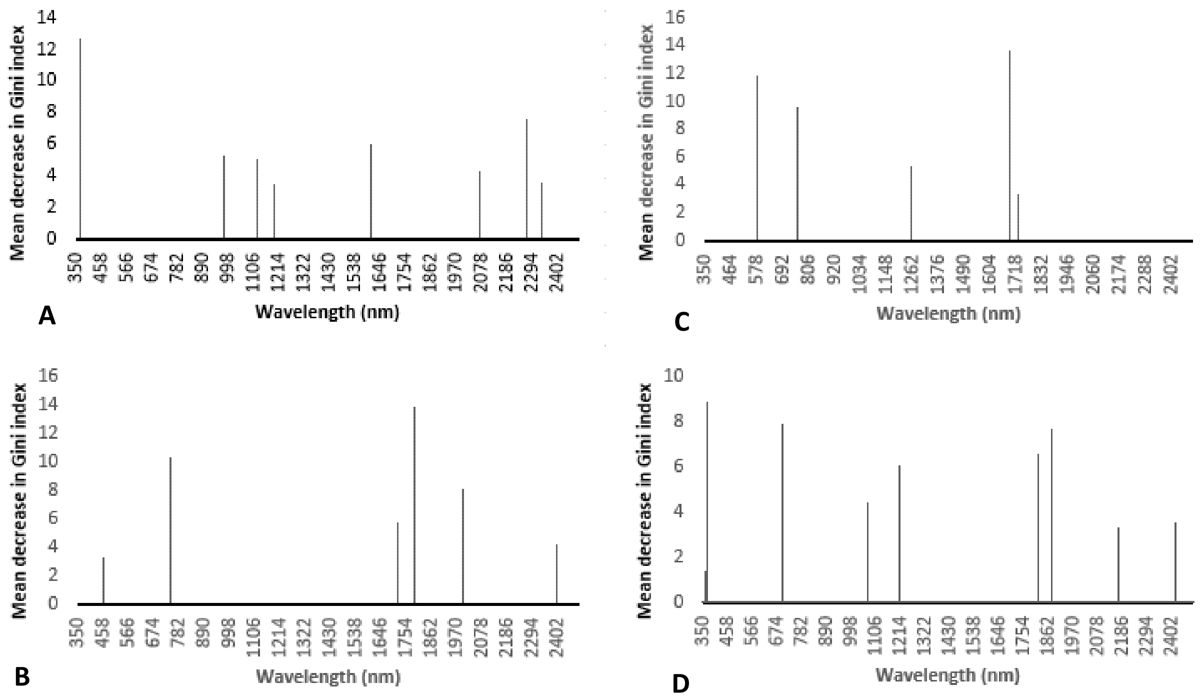

Figure 0.2 Selected wavelengths measured by GGRF using mean decrease in Gini Index for distinguishing between (A) AD_C and PA_C under controlled conditions, (B) AD_T and PA_T post treatment, (C) AD_T under controlled conditions and AD_T post treatment. (D) AD_T under controlled conditions and AD_T post treatment.

4.3 Classification using Random Forest

The GRRF identified importance wavelengths served as input variables for the RF classifier in order to distinguish between the control and treated plants. Tables 4.3.1 and 4.3.2 display the results obtained from the GRRF analysis. The OA of the classifier, calculated as the proportion of correctly classified samples to the total sum of samples across both classes, reveals a notable difference when discriminating between the control and treated plant species of *A. donax* and *P. australis*. Table 4.3.1 shows this difference, indicating an improvement in overall accuracy when the plant species are subjected to treatment.

Specifically, the overall accuracy for plant species exposed to copper and acid treatment is notably higher at 83.5% (OOB estimate of error rate: 16.48%), compared to 76.1% (OOB estimate of error rate: 23.88%) for plant species grown under controlled conditions. This improvement underscores the effectiveness of the classifier when discriminating between the two conditions, particularly with the application of treatment. In line with the OA findings, both the PA and UA exhibit superior values when distinguishing between species exposed to treatment compared to those grown under controlled conditions. Table 4.3.2 shows confusion matrix results when discriminating between *A. donax* and *P. australis* under control and treatment conditions. The overall accuracy of discriminating A. donax, between control and treated species is determined to be 56.6%, slightly surpassing that of *P. australis* discrimination, which stands at 55.7%. Consequently, the out-of-bag (OOB) error rates for discriminating *A. donax* and *P. australis* under control and treated conditions are calculated to be 43.43% and 44.32%, respectively. The Kappa coefficients for when plants are under control and when under treatment are high, especially when they are under treatment. The kappa of AD_C and AD_T and that of PA_C and PA_T species are relatively low, indicating a slight agreement.

Table 4.3. 1: Confusion matrix showing OA, UA, PA of AD_C and PA_C under controlled conditions, and AD_T and PA_T post treatment.

A. donax (AD_C) and *P. australis* (PA_C)					*A. donax* (AD_T) and *P. australis* (PA_T)				
	AD_C	PA_C	Total	UA (%)		AD_T	PA_T	Total	UA (%)
AD_C	30	7	37	81	AD_T	39	8	47	83.0
PA_C	9	21	30	70	PA_T	7	37	44	84.1
Total	39	28	67		Total	46	45	91	
PA (%)	76.9	75			PA (%)	84.8	82.2		
Overall Accuracy 76.1% Kappa: 0.51					Overall Accuracy: 83.5% Kappa: 0.67				

Table 0.1 Confusion matrix showing OA, UA, and PA of AD_T and AD_T post treatment, and AD_T and AD_T post treatment.

A. donax (AD_C) and *A. donax* (AD_T)					*P. australis* (PA_C) and *P. australis* (PA_T)				
	AD_C	PA_T	Total	UA (%)		PA_C	PA_T	Total	UA (%)
AD_C	33	19	52	63.5	PA_C	24	20	44	54.5
AD_T	24	23	47	48.9	PA_T	19	25	44	56.8
Total	57	42	99		Total	43	45	88	
PA (%)	57.9	54.8			PA (%)	55.8	55.6		
Overall Accuracy 56.6% Kappa: 0.12					Overall Accuracy 55.7% Kappa: 0.11				

4.4 Resampling to Multispectral and Hyperspectral Sensors

The original in situ hyperspectral data underwent a resampling process to align with the spectral characteristics HyMap, WorldView-3, WorldView-2, and Sentinel-2. This resampled dataset was then subjected to classification using the Random Forest (RF) classifier. The primary objective was to evaluate the RF classifier's effectiveness in distinguishing between the two plant species, *A. donax* and *P. australis*, under different conditions—when subjected to treatment and when under control conditions. The results are aligned below.

4.4.1 Resampling to HyMap

Figure 4.4.1 below shows the profile of the HyMap resampled hyperspectral signature and it is similar to the original hyperspectral data used for resampling. Spectral discrimination between the control and treated species is seen on the whole electromagnetic spectrum. However, there is a sharp decrease after the near shortwave-infrared.

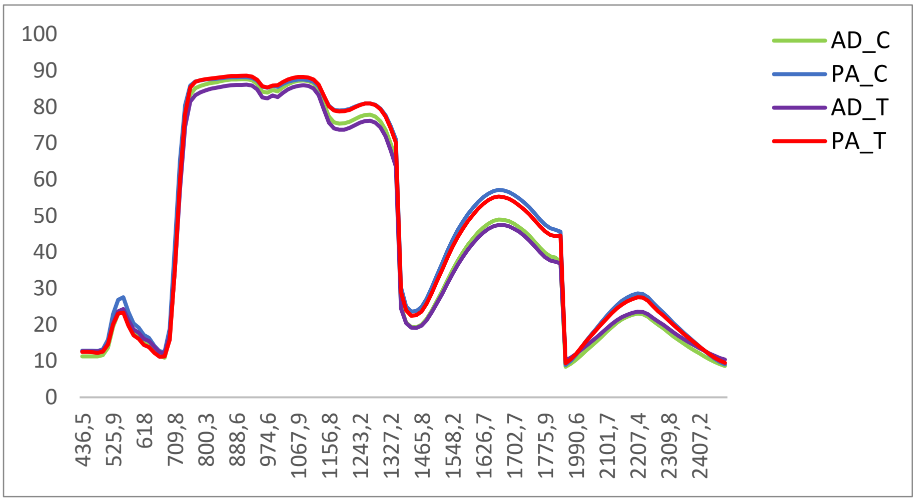

Figure 0.1 Hyperspectral reflectance of AD_T and PA_T before and post treatment.

Table 4.4.1 and Table 4.4.2 show the confusion matrix of HyMap resampled *A. donax* and *P. australis* when under control and when exposed to treatment. The overall accuracy of the *A. donax* and *P. australis* when grown under treatment conditions is higher (83.5%) than when the species are grown under control conditions (72.9%). The obtained pattern is similar to that of the in-situ field spectra obtained above. The overall accuracy of the species when grown under treatment conditions is equivalent in both the in situ hyperspectral data and resampled HyMap. On the other hand, the situ hyperspectral data was able to discriminate the species when grown under control conditions better. The OA in discriminating between *A. donax* control and treatment is 59.6%, and *P. australis* control and treated species is 62.5%. OA of resampled HyMap show that it was better in discriminating both the *A. donax* and *P. australis* under control and treatment compared to the original hyperspectral data. When species are under control (AD_C and PA_C), the model achieved a high UA of 76.9% for AD_C and 68.2% for PA_C, and these are subsequently lower than the obtained user's accuracy before resampling. The UA when discriminating the species under treatment are 80% and above, both before and after resampling. The user's accuracy when discriminating *A. donax* control and treatment and *P. australis* control and treated species is better when using resampled HyMap compared to the original in situ hyperspectral data. The producer's accuracy of *A. donax* and *P. australis* under control is higher after resampling. This is true when discriminating *A. donax* control and treatment, and *P. australis* control and treated species as well.

Table 0.1 Confusion matrix showing resampled HyMap OA, UA, PA of AD_C and PA_C under controlled conditions, and AD_T and. PA_T post treatment.

A. donax (AD_C) and P australis (PA_C)				
	AD_C	PA_C	Total	UA (%)
AD_C	40	12	52	76.9
PA_C	14	30	44	68.2
Total	54	42	96	
PA (%)	74.1	71.4		
Overall Accuracy: 72.9% Kappa: 0.45				

A. donax (AD_T) and P australis (PA_T)				
	AD_T	PA_T	Total	UA (%)
AD_T	41	6	47	87.2
PA_T	9	35	44	79.5
Total	50	41	91	
PA (%)	82.0	85.4		
Overall Accuracy: 83.5% Kappa: 0.67				

Table 0.2 Confusion matrix showing resampled HyMap OA, UA, PA of AD_T and AD_T post treatment, and AD_T and AD_T post treatment.

A. donax (AD_C) and P australis (AD_T)					*A. donax* (PA_C) and P australis (PA_T)				
	AD_C	AD_T	Total	UA (%)		AD_T	PA_T	Total	UA (%)
AD_C	34	18	52	81	PA_C	26	18	44	59.1
AD_T	22	25	47	70	PA_T	15	29	44	65.9
Total	56	43	99		Total	41	47	88	
PA (%)	76.9	75			PA (%)	63.4	61.7		
Overall Accuracy 59.6% Kappa: 0.19					Overall Accuracy 62.5% Kappa: 0.25				

4.4.2 Resampling to WorldView-3

Figure 4.4.2 shows the spectral reflectance of WorldView-3 resampled data. The spectral reflectance differs slightly from the hyperspectral spectra. There is a shift in the REP and the NIR region is narrower.

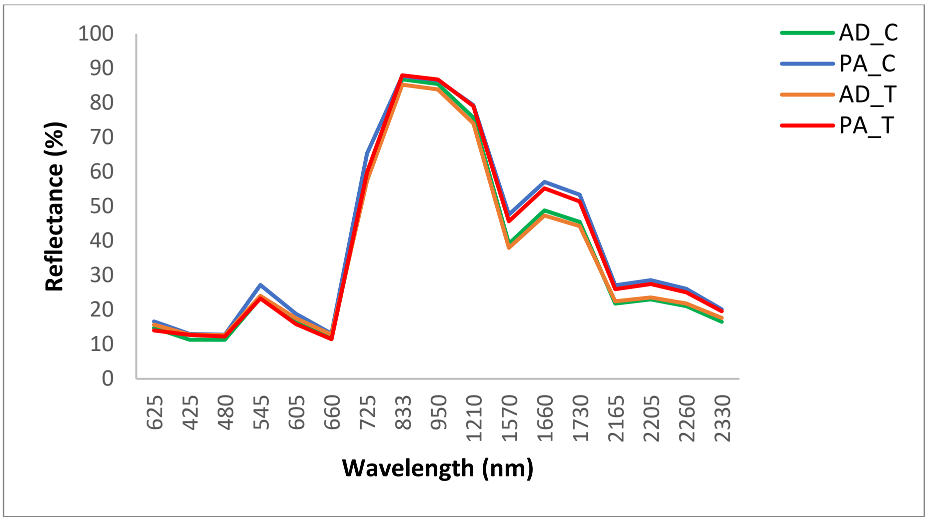

Figure 0.2 Hyperspectral reflectance of AD_T and PA_T before and post treatment.

The accuracy assessments in Table 4.4.2 and Table 4.4.3 reveal the classification performance of the model in distinguishing between two plant species, *A. donax* (AD) and *P. australis* (PA), under both control (AD_C and PA_C) and treatment (AD_T and PA_T) conditions. The overall accuracy for discriminating between both species under control conditions is 78.1% and for discriminating after treatment (AD_C and AD_T) is 84.6%. There is a 2% and 1.1% increase in the overall accuracies for when discriminating the species under control and after treatment, respectively. Table 4.4.2.2 shows an accuracy assessment table that differentiate between *A. donax* and *P. australis* under control (AD_C and PA_C) and treatment (AD_T and PA_T) conditions. The overall accuracy for discriminating between AD_C and AD_T is 55.6% and for discriminating between PA_C and PA_T is 60.2%. The obtained accuracies show that resampled WorldView-3 is better at discriminating between AD_C and AD_T than the original data. For the control conditions, the model achieved a UA of 78.85% for *A. donax* (AD_C) and 77.27% for *P. australis* (PA_C), demonstrating its effectiveness in correctly distinguishing these species under control conditions.

A better UA when discriminating *A. donax* (AD_C) was obtained for the WorldView-3 resampled data, in comparison to the original hyperspectral data. However, the contrast is true for *P. australis* (PA_C) user's accuracy. Under treatment conditions, the model exhibited a user's accuracy of 83.0% for AD_T and 86.4% for PA_T, which has values close to the original data. Moreover, for the discrimination between AD_C and AD_T, the user's accuracy is 63.5% for correctly predicting *P. australis* under treatment conditions and 46.8% for correctly predicting *A. donax* under treatment conditions. The obtained user's accuracies for hyperspectral and resampled WorldView-3 are relative to one another. The producer's accuracy for AD_C and PA_C is 80.4% and 75.6%, respectively; and for the species under treatment conditions, it is 83.0 and 86.4 for AD_T and PA_T, respectively. This shows that the resampled WorldView-3 was better at discriminating between the PA of both the species under control and treatment conditions.

Table 0.3 Confusion matrix showing resampled WorldView-3 OA, UA, PA of AD_C and PA_C under controlled conditions, and AD_T and PA_T post treatment.

A. donax (AD_C) and P australis (PA_C)					*A. donax* (AD_T) and P australis (PA_T)				
	AD_C	PA_C	Total	UA (%)		AD_T	PA_T	Total	UA (%)
AD_C	41	11	52	78.8	AD_T	39	8	47	83.0
PA_C	10	34	44	77.3	PA_T	6	38	44	86.4
Total	51	45	96		Total	45	46	91	
PA (%)	80.4	75.6			PA (%)	86.7	82.6		
Overall Accuracy 78.1% Kappa: 0.53					Overall Accuracy 84.6% Kappa: 0.69				

Table 0.4 Confusion matrix showing OA, UA, PA of AD_T and AD_T post treatment, and AD_T and AD_T post treatment.

A. donax (AD_C) and P australis (AD_T)					*A. donax* (PA_C) and P australis (PA_T)				
	AD_C	AD_T	Total	UA (%)		PA_C	PA_T	Total	UA (%)
AD_C	33	19	52	63.5	PA_C	26	18	44	59.1
AD_T	25	22	47	46.8	PA_T	17	27	44	61.4
Total	58	41	99		Total	43	45	88	
PA (%)	56.9	53.7			PA (%)	60.5	60		
Overall Accuracy 55.6% Kappa: 0.10					Overall Accuracy 60.2% Kappa: 0.20				

4.4.3 Resampling to WV2

Figure 4.4.3 shows the resampled WorldView-2 spectral reflectance. However, the spectral range is different from the original hyperspectral data. The REP is identified in the lower bound and has shifted and the near-infrared and shortwave-infrared are not present.

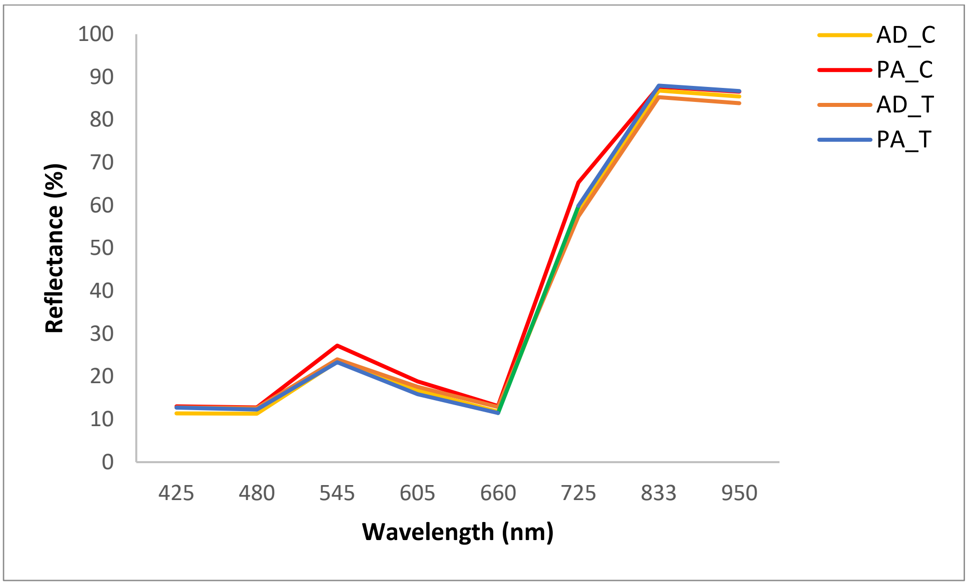

Figure 0.3 Hyperspectral reflectance of AD_T and PA_T before and post treatment.

Table 4.4.5 and Table 4.4.6 show the performance of RF model in distinguishing between *A. donax* (AD) and *P. australis*. For when both the species are under control (AD_C and PA_C) and treatment (AD_T and PA_T), the model achieved an overall accuracy of 65.6% and 78%, respectively. There is a huge decrease in the overall accuracies of the abovementioned, compared to the original in situ hyperspectral. For the discrimination between AD_C and AD_T, the model achieved an overall accuracy of 52.5% which is poor compared to the original data. However, the is an improvement in the overall accuracy between PA_C and PA_T, demonstrating the ability of the resampled WV2 sensor in discriminating between PA_C and PA_T using the RF classifier. A UA of 71.2% for AD_C and 59.1% for PA_C was achieved when classifying the control species.

In the treatment conditions (AD_T and PA_T), UA is 61.5% for AD_C and 59.1% for PA_C. The obtained UA for resampled WV2 were poor compared to the original hyperspectral data before resampling. The UA when discriminating AD_C and AD_T and PA_C and PA_T is 61.5% and 42.6%, and 61.4% and 59.1%, respectively. There is an improvement in the in the accuracies of *P. australis* while there is no improvement in *A. donax* species. There was a decrease in producer's accuracies for species when they are in both control and treatment conditions. For the discrimination between AD_C and AD_T, the model achieved a PA of 54.2% for AD_C and 50% for AD_T, and in discriminating between PA_C and PA_T, the producer's accuracy was 60% for PA_T and 60.5% for PA_C. There is no improvement in the accuracies when using resampled WV2 data in the discriminating of the species, using the RF classifier.

Table 0.5 Confusion matrix showing resampled WorldView-2 OA, UA, PA of AD_C and PA_C under controlled conditions, and AD_T and PA_T post treatment.

A. donax (AD_C) and P australis (PA_C)					*A. donax* (AD_T) and P australis (PA_T)				
	AD_C	PA_C	Total	UA (%)		AD_T	PA_T	Total	UA (%)
AD_C	37	15	52	71.2	AD_T	37	10	47	78.7
PA_C	18	26	44	59.1	PA_T	10	34	44	77.3
Total	55	41	96		Total	47	44	91	
PA (%)	67.3	63.4			PA (%)	78.7	77.3		
Overall Accuracy 65.6% Kappa: 0.30					Overall Accuracy 78% Kappa: 0.56				

Table 0.6 Confusion matrix showing OA, UA, PA of AD_C and AD_T post treatment, and PA_C and AD_T post treatment.

A. donax (AD_C) and P australis (AD_T)					*A. donax* (PA_C) and P australis (PA_T)				
	AD_C	AD_T	Total	UA (%)		PA_C	PA_T	Total	UA (%)
AD_C	32	20	52	61.5	PA_C	27	17	44	61.4
AD_T	27	20	47	42.6	PA_T	18	26	44	59.1
Total	59	40	99		Total	45	43	88	
PA (%)	54.2	50			PA (%)	60	60.5		
Overall Accuracy 52.5% Kappa: 0.04					Overall Accuracy 60.2% Kappa: 0.2				

4.4.4 Resampling to Sentinel 2

The spectral signature of the resampled Sentinel 2 profile is similar to that of the original hyperspectral reflectance as shown in Figure 4.4.4. However, the shortwave-infrared region is shorter compared to the original hyperspectral signature. There is also a peak on the species green reflection and a shift in the red edge.

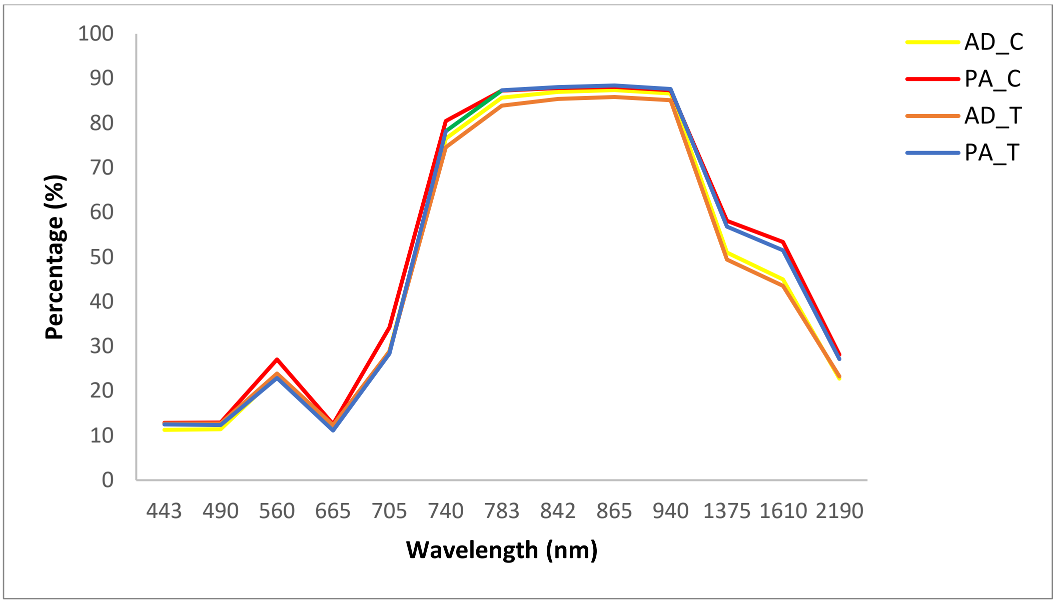

Figure 0.4 Hyperspectral reflectance of AD_T and PA_T before and post treatment.

Tables 4.4.7 and 4.4.8 present the evaluation of the Random Forest (RF) model's performance in distinguishing between *A. donax* (AD) and *P. australis*. In the context of control (AD_C and PA_C) and treatment (AD_T and PA_T) conditions, the RF model achieved overall accuracies of 65.6% and 78%, respectively. Notably, there was a significant decrease in OA compared to the original in situ hyperspectral reflectance, especially for AD_C and AD_T. While discrimination between PA_C and PA_T demonstrated the ability of the resampled Sentinel 2 sensor to enhance accuracy using the RF classifier, AD_C and AD_T showed poor results. User's accuracy (UA) for AD_C and PA_C under control conditions was 71.2% and 59.1%, respectively, with similar trends observed in treatment conditions. Producer's accuracies showed a decrease for both species under control and treatment conditions. Discriminating between AD_C and AD_T displayed poor producer's accuracy (54.2% for AD_C and 50% for AD_T), while PA_C and PA_T demonstrated some improvement but remained suboptimal.

Table 0.7 Confusion matrix showing resampled Sentinel 2 OA, UA, PA of AD_C and PA_C under controlled conditions, and AD_T and PA_T post treatment.

A. donax (AD_C) and P australis (PA_C)					*A. donax* (AD_T) and P australis (PA_T)				
	AD_C	PA_C	Total	UA (%)		AD_T	PA_T	Total	UA (%)
AD_C	26	18	44	59.1	AD_T	37	10	47	78.7
PA_C	19	25	44	56.8	PA_T	7	37	44	84.1
Total	45	43	88		Total	44	47	91	
PA (%)	57.8	58.1			PA (%)	84.1	78.7		
Overall Accuracy 58.0% Kappa: 0.16					Overall Accuracy 81.3% kappa: 0.63				

Table 0.8 Confusion matrix showing resampled Sentinel 2 OA, UA, PA of AD_C and AD_T post treatment, and PA_C and PA_T) post treatment.

A. donax (AD_C) and P australis (AD_T)					*A. donax* (PA_T) and P australis (PA_T)				
	AD_C	AD_T	Total	UA (%)		AD_T	PA_T	Total	UA (%)
AD_C	30	22	52	57.7	AD_T	26	18	44	59.1
AD_T	24	23	47	48.9	PA_T	19	25	44	56.8
Total	54	45	99		Total	45	43	91	
PA (%)	55.6	51.1			PA (%)	57.8	58.1		
Overall Accuracy 53.5% Kappa: 0.07					Overall Accuracy 56.0% Kappa: 0.16				

4.5 Red Edge Position

Using the LFI technique, the REP for control and treated *Phragmites australis (Cav.)* is 719 nm and 717 nm, respectively. Both the healthy and unhealthy *Phragmites australis* species show more dominance in the NIR region. There is no shift in the REP (719) for the *Arundo donax L.* species, irrespective of whether they are under control or exposed to treatment. Moreover, high dominance is also shown in the NIR region.

CHAPTER FIVE: DISCUSSION AND CONCLUSION

This study aims to investigate the spectral characteristics of *Arundo donax L.* and *Phragmites australis* (Cav.) species, focusing on spectrally discriminating between them under controlled conditions and conditions involving exposure to heavy metals. The objectives include discriminating between the two species, assessing the discriminatory potential of resampled data from different sensors, and analysing shifts in the red edge position under varying environmental conditions. The study has shown a spectral significance between the two species when they are under control and treatment conditions. It further gave good accuracy assessments of resampled data, illustrating the potential of these sensors to be used in discriminating the two species. The study will help understand wetland vegetation and improve environmental monitoring using RS. Based on the results, the discussion will look at the analysis of copper and species spectral characteristics, feature importance selection measurement, and classification using random forest. It will further discuss results obtained from resampling and the shift in the REP.

5.1 Analysis of Copper

The spectral reflectance of light is influenced by the interaction of the EMS with the components of the plant, such as the pigments and hydro content (Li *et al.*, 2023). When a plant is under stress conditions, the leaves have lower reflectance values than healthy ones. Hence, the spectral signature of the species changed when they were under controlled conditions and after copper and acid conditions. The spectral signatures decreased notably in the NIR and near SWIR regions for *A. donax* and decreased in the visible and near SWIR regions for *Phragmites australis*. These results are comparable to the results found by (Raypah *et al.*, 2024), where the reflectance of plant species decreased with days, since introduced to stressed. The decrease in the near infrared for *A. donax* aligns with other studies (Azmi *et al.*, 2021; Liaghat *et al.*, 2014). The cellular composition of leaves primarily influences the reflected light within the NIR range. So, it may be assumed that the cell structure of Arundo donax was fractured compared to those of *Phragmites australis*. Both plant species had a higher copper level in the soil than in water, possibly because reeds are tolerant to elevated metals in the soil (Delplace *et al.*, 2020). *P. australis* and *A. donax* can also immobilise or contain heavy metals in the soil (Pérez-Sirvent *et al.*, 2017; Castaldi *et al.*, 2017). Guo *et al.* (2014) also found that the amounts of Fe, Mn, and Al in the roots of PA were closely linked to the levels of these elements in the soil when used in acid mine contaminated areas.

5.2 Feature Importance Selection Measurement

Although hyperspectral data enhances the ability to distinguish between vegetation by leveraging their biochemical and structural characteristics (Taylor *et al.*, 2012), it introduces high-dimensional complexity. Using this type of data may prolong the amount of time taken for classification reducing efficiency (Zhou *et al.*, 2021). Feature selection was employed to extract the most suitable feature subset, enhancing classification outcomes with a reduced number of features (Gau *et al.*, 2023). The default 500 trees were used to achieve high accuracy. Huang *et al.* (2016) state that a larger number of trees results in higher precision accuracy. The RF feature selection technique successfully selected the important bands in the electromagnetic spectrum. The selected bands for the different species and conditions varied across the spectrum. When both species were under control, the selected bands were found across the whole spectrum. Important bands were also found across the whole spectrum when *Arundo donax L.* (AD_T) is under controlled conditions, post-treatment of *Arundo donax L.* (AD_T) and when *Phragmites australis* (Cav.) (PA_T) is under controlled conditions, and *Phragmites australis* (AD_T) post-treatment. However, after the species were treated, there was a gap in the NIR and important bands were found in the visible, REP and on shortwave-infrared. Earlier research indicated that green leaves exhibit the most significant variability in the VIR, REP, and near-infrared regions, potentially leading to the identification of crucial wavelengths within these regions (Mansour *et al.*, 2012; Beyer *et al.*, 2019). While this holds true for the findings in the present study, it's noteworthy that the shortwave-infrared spectrum also contains important wavelengths.

The REP was selected in groups where one or both the plants were treated, but not when the species were both under control conditions. This may be due to the stress posed by the treatment of the plants. According to Chiarito *et al.* (2020), the REP experiences the most significant shift in slope in the vegetation's reflectance spectral signature as it provides insights into vegetation stress, levels of chlorophyll, and nitrogen status. The blue bands are also important, and this may be attributed to their relation to chlorophyll b absorption (Chiarito *et al.*, 2020). Even though most studies state that the visible, REP and NIR regions are the most important, the SWIR regions were also important in this study. The SWIR region provides data regarding the presence of water and the mass of the leaf, thus exhibiting correlation with LAI and biomass (Psomas *et al.,* 2011). This means the treatment may influence the species' biomass. Moreover, Adam *et al.* (2012) state that studies that utilized remotely sensed data for wetland vegetation classification have indicated the significant role of short-wave infrared in distinguishing between wetland species.

5.3 Species Classification Using Random Forest

An accuracy of 76.1% and 83.5% was obtained when both the species were under control and after the copper and acid treatment, respectively. This means the species were better discriminated against when exposed to the treatment. This is because Arundo donax and *Phragmites australis* are morphologically similar and occur in similar habitats (Ollendorf *et al.*, 1998; Guthrie, 2007). Tesfamichael (2017) states that morphological characteristics may contribute to spectral similarity. For example, Fernandes *et al.* (2013) successfully differentiated *A. donax* from other species; however, they faced challenges distinguishing phragmites, as only a few wavelengths set the two species apart. The model was not effective in discriminating *Arundo donax L.* (AD_T) under controlled conditions and *Arundo donax L.* (AD_T) post-treatment (56.6% overall accuracy). It was also not effective in discriminating *P. australis* (PA_T) when under controlled conditions and post-treatment (55.7% overall accuracy).

5.4 Resampling to Multispectral and Hyperspectral Sensors

Resampled HyMap showed an excellent similarity with ASD ground reflectance. At the same time, the other resampled spectra were less precise and more generalized but still retained the same pattern of the original spectra except for spectra simulated to WorldView-2. The peak in the visible green band (540-560nm) and the rapid increase in the REP (670-780) persisted in all the resampled data, maintaining a similar reflectance in the VIR area. This is as a result of the green reflectance of the species and the change in the REP. The minimal influence of scattering effects on this spectral range can explain this phenomenon (Chakouri *et al.*, 2020). When discriminating both species under control conditions, the accuracy of resampled HyMap was reduced; when both species were treated, the accuracy remained the same as before resampling. This may be due to the fact that airborne hyperspectral data typically offer high spectral resolution but relatively lower spatial resolution, resulting in limitations in predicting vegetation biochemical traits compared to field spectrometer sensors (Hassani *et al.*, 2023). This illustrates the compromise between the clarity of detail and the ability to distinguish between different wavelengths in RS data. However, when discriminating the species distinctively- when they are healthy and unhealthy- resampled HyMap significantly improved the overall accuracy. Resampled HyMap also showed a remarkable accuracy of 96% in a study by Adam *et al.* (2012) when discriminating *Phragmites australis*, showing significant potential for the HyMap to discriminate the species.

Resampled HyMap and WorldView-3 gave very similar results to the original results, and this is due to the number and types of bands that these satellites have. They cover the spectrum's visible, near-infrared, and shortwave-infrared regions (Mutanga *et al.*, 2009). Moreover, HyMap data has more than 100 bands covering a broad electromagnetic spectrum, while WV-3 has 16 bands. This shows the potential of using these sensors for discriminating the species. Compared to HyMap and WV 3; WV 2 and Sentinel 2 have 8 and 12 bands, respectively. Even though WV 2 and Sentinel 2 have red bands and NIR regions, which helps with plant discrimination. The infrared region of WV 2 and Sentinel 2 is limited compared to the other two sensors. This could be due to the findings of Tesfamichael *et al.* (2017), who suggest that longer wavelength bands allow for an effective distinguishing of vegetations. Govender *et al.* (2009) and Holzman *et al.* (2021) also state that the SWIR region is sensitive to leaf water content and making them well-suited for evaluating the presence of water in herbaceous plants. The importance band of the species were primarily found in the SWIR region in the original data, meaning the region is sensitive to discrimination.

The lower accuracy observed for Sentinel 2 may stem from the absence of spectral coverage in the SWIR II region and limited spectral resolution in the SWIR and region. Ferner *et al.* (2021) similarly discovered that the limited broad bands in the SWIR region of Sentinel-2 decreased the predictive capability of numerous forage models in comparison to those based on hyperspectral data. Adagbasa *et al.* (2019) also concluded that reduced accuracies were likely due to the spectral resolution of 60 m. Even though Sentinel 2 had low overall accuracies for other species combinations, the overall accuracy was high when both the species were treated with acid and copper. This may be because of the change in the two species' morphological characteristics and the sensitivity in the REP. The Red edge band can assess chemical elements of the plant and its health and also discriminate vegetation species (Odindi *et al.,* 2017). Lastly, the upscaling to airborne sensors may present some problems due to atmospheric absorption and noise in the blue region of the spectrum (Adam *et al.,* 2012).

5.5 Red Edge Position

Increased concentration of HMs in the soil can reduce vegetation growth, including reduced chlorophyll content and altered leaf internal structure (Fu *et al.*, 2020). These changes may consequently cause a shift in the REP, directly or indirectly influencing the spectral characteristics of plants (Wu *et al.,* 2019). When

Phragmites australis was exposed to copper and acid treatment, a slight shift of 2 nm towards shorter wavelengths was observed. This shift aligns with the findings of Zhai *et al.* (2023), indicating that a movement of the REP to shorter wavelengths indicates stress conditions in vegetation. These findings are consistent with the findings from Deventer and Cho (2013). They discovered the average REP values for leaves during winter were 708 nm at the contaminated sites, while the control site showed a REP of 716 nm.

On the other hand, there was no shift in the REP (719) of Arundo donax., regardless of whether it was under controlled or treatment conditions. The REP in vegetation spectral reflectance serves as an indirect indicator of vegetation chlorophyll content. (Frampton *et al.,* 2013). Therefore, we may assume the copper and acid treatment did not influence the plant's chlorophyll content and, consequently, the plant's health. These results are similar to those of Papazoglou and Boura (2005), who did not find any statistical significance when Arundo donax species were under control and when under treatment (Chlorophyll content values ranged between 46.3 and 57.0) (Papazoglou and Boura, 2005). According to Nuwete (2013), the red edge position of healthy plants normally stabilized at wavelengths of about 712- 715 nm. Therefore, we may conclude that, regardless of the treatment, the species could still be classified under good conditions.

This study investigated the spectral response of *Arundo donax* and *Phragmites australis* under copper and acid treatment. Significant shifts in spectral signatures were observed, particularly in the NIR and SWIR regions for *A. donax* and in the visible and near shortwave-infrared regions for *P. australis*. Random Forest classification demonstrated improved discrimination accuracy (83.5%) post-treatment compared to control conditions (76.1%). This shows that these similar species were discriminated against better after treatment conditions than when they were healthy. Feature importance analysis highlighted the significance of shortwave-infrared regions, contrary to the common emphasis on visible and near-infrared regions. Resampling of hyperspectral data, especially HyMap and WV 3, showed promise for discriminating between the species. The red edge position analysis indicated stress-induced shifts in *P. australis*, while *A. donax* remained stable, suggesting resilience. The study's limitation is the lack of chlorophyll content and copper concentration data for both species under control and treatment conditions.

It is recommended that the consistency of classification using actual satellite hyperspectral and multispectral sensors data for discrimination of the species under the two different conditions is tested.

References

Abeer, N., Khan, S.A., Muhammad, S., Rasool, A. and Ahmad, I. 2020. Health risk assessment and provenance of arsenic and heavy metal in drinking water in Islamabad, Pakistan. *Environmental technology & innovation*, *20*: pp.1-8.

Adagbasa, E.G., Adelabu, S.A. and Okello, T.W. 2022. Application of deep learning with stratified K-fold for vegetation species discrimation in a protected mountainous region using Sentinel-2 image. *Geocarto International*, *37*(1): pp.142-162.

Adam, E.M., Mutanga, O., Rugege, D. and Ismail, R. 2012. Discriminating the papyrus vegetation (Cyperus papyrus L.) and its co-existent species using random forest and hyperspectral data resampled to HYMAP. *International Journal of Remote Sensing*, *33*(2): pp.552-569.

Addo-Bediako, A., Nukeri, S. and Kekana, M. 2021. Heavy metal and metalloid contamination in the sediments of the Spekboom River, South Africa. *Applied Water Science*, *11*: pp.1-9.

Adeeyo, Adeyemi O. Stanley S. Ndlovu, Linda M. Ngwagwe, Mulalo Mudau, Mercy A. Alabi, and Joshua N. Edokpayi. 2022. Wetland Resources in South Africa: Threats and Metadata Study. *Resources*, https://doi.org/10.3390/resources11060054

Adhikary, S., Biswas, B., Naskar, M., Mukherjee, B., Singh, A., & Atta, K. 2023. Remote sensing for agricultural applications: a meta-review. *Remote Sensing of Environment*, doi: https://doi.org/10.5772/intechopen.106876

Aerts, R., Verhoeven, J.T.A. and Whigham, D.F. 1999. Plant-mediated controls on nutrient cycling in temperate fens and bogs. Ecology, 80(7): pp.2170-2181.

Al-Homaidan, A.A., Al-Otaibi, T.G., El-Sheikh, M.A., Al-Ghanayem, A.A. and Ameen, F., 2020. Accumulation of heavy metals in a macrophyte *Phragmites australis*: implications to phytoremediation in the Arabian Peninsula wadis. *Environmental Monitoring and Assessment*, *192*: pp.1-10.

Ali, A. and Imran, M., 2020. Evaluating the potential of red edge position (REP) of hyperspectral remote sensing data for real time estimation of LAI & chlorophyll content of kinnow mandarin (Citrus reticulata) fruit orchards. *Scientia Horticulturae*, *https://doi.org/10.1016/j.scienta.2020.109326*

Ali, A., Imran, M., Ali, A. and Khan, M.A., 2022. Evaluating Sentinel-2 red edge through hyperspectral profiles for monitoring LAI & chlorophyll content of Kinnow Mandarin orchards. *Remote Sensing Applications: Society and Environment*, *https://doi.org/10.1016/j.rsase.2022.100719*

Ali, H. and Khan, E. 2018. What are heavy metals? Long-standing controversy over the scientific use of the term ‘heavy metals’ – proposal of a comprehensive definition. Toxicological & Environmental Chemistry, 100(1): pp. 6-19.

An, S. and Verhoeven, J.T., 2019. Wetland functions and ecosystem services: Implications for wetland restoration and wise use. In An, S., Verhoeven, J. (Eds.). Wetlands: Ecosystem Services, Restoration and Wise Use. Switzerland: Springer International Publishing: pp. 1-10.

Ao, M., Chen, X., Deng, T., Sun, S., Tang, Y., Morel, J.L., Qiu, R. and Wang, S. 2022. Chromium biogeochemical behaviour in soil-plant systems and remediation strategies: A critical review. *Journal of Hazardous Materials*, *https://doi.org/10.1016/j.jhazmat.2021.127233*

Arellano, P., Tansey, K., Balzter, H. and Boyd, D.S. 2017. Field spectroscopy and radiative transfer modelling to assess impacts of petroleum pollution on biophysical and biochemical parameters of the Amazon rainforest. *Environmental Earth Sciences*, *76*: pp.1-14.

Aryal, K., Ojha, B.R. and Maraseni, T. 2021. Perceived importance and economic valuation of ecosystem services in Ghodaghodi wetland of Nepal. *Land Use Policy*, https://doi.org/10.1016/j.landusepol.2021.105450

Asati, A., Pichhode, M. and Nikhil, K. 2016. Effect of heavy metals on plants: an overview. *International Journal of Application or Innovation in Engineering & Management*, *5*(3): pp.56-66.

Asrari, E. 2014. Heavy metals in contaminated soils: a review of sources, chemistry, risks, and best available strategies for remediation. Wiley and Sons, doi: https://doi.org/10.1201/b16566-7

Atanassova, B. and Zapryanova, N. 2009. Influence of heavy metal stress on growth and flowering of Salvia splendens Ker.-Gawl. *Biotechnology & Biotechnological Equipment*, *23*(1): pp.173-176.

Azizi, A., Krika, A. and Krika, F. 2020. Heavy metal bioaccumulation and distribution in Typha latifolia and Arundo donax: implication for phytoremediation. *Caspian Journal of Environmental Sciences*, *18*(1): pp.21-29.

Azmi, A.N.N., Khairunniza-Bejo, S., Jahari, M., Muharram, F.M. and Yule, I. 2021. Identification of a suitable machine learning model for detection of asymptomatic Ganoderma boninense infection in oil palm seedlings using hyperspectral data. *Applied Sciences*, *https://doi.org/10.3390/app112411798*

Balafrej, H., Bogusz, D., Triqui, Z.E.A., Guedira, A., Bendaou, N., Smouni, A. and Fahr, M. 2020. Zinc hyperaccumulation in plants: A review. *Plants*, *9*(5): p.562.

Balali-Mood, M., Naseri, K., Tahergorabi, Z., Khazdair, M.R. and Sadeghi, M. 2021. Toxic mechanisms of five heavy metals: mercury, lead, chromium, cadmium, and arsenic. *Frontiers in Pharmacology*, doi: 10.3389/fphar.2021.643972 .

Balwan, W.K. and Kour, S. 2021. Wetland-an ecological boon for the environment. *East African Scholars Journal of Agriculture and Life Sciences*, 4(3): pp.38-48.

Bateganya, N.L., Nakalanzi, D., Babu, M. and Hein, T. 2015. Buffering municipal wastewater pollution using urban wetlands in sub-Saharan Africa: a case of Masaka municipality, Uganda. *Environmental Technology*, *36*(17): pp.2149-2160.

Beck, K.G., Zimmerman, K., Schardt, J.D., Stone, J., Lukens, R.R., Reichard, S., Randall, J., Cangelosi, A.A., Cooper, D. and Thompson, J.P. 2008. Invasive species defined in a policy context: Recommendations from the Federal Invasive Species Advisory Committee. *Invasive Plant Science and Management*, *1*(4): pp.414-421.

Bedane, G.A., Feyisa, G.L. and Wakjira, F.S. 2023. Modeling effects of abiotic factors on the abundances of eight woody species in the Harana forest using artificial networks, random forest, and generalized linear models. *Ecological Processes*, *12*(1): pp.10.

Behmann, J., Mahlein, AK., Paulus, S. *et al.* Generation and application of hyperspectral 3D plant models: methods and challenges. *Machine Vision and Applications* , doi: https://doi.org/10.1007/s00138-015-0716-8

Bello, A.O., Tawabini, B.S., Khalil, A.B., Boland, C.R. and Saleh, T.A. 2018. Phytoremediation of cadmium-, lead-and nickel-contaminated water by *Phragmites australis* in hydroponic systems. *Ecological Engineering*, *doi: http://dx.doi.org/10.1016/j.ecoleng.2018.05.035*

Benavides, M.P., Gallego, S.M. and Tomaro, M.L. 2005. Cadmium toxicity in plants. *Brazilian Journal of Plant Physiology*, *17 (1)*: pp.21-34.

Beyer, F., Jurasinski, G., Couwenberg, J. and Grenzdörffer, G. 2019. Multisensor data to derive peatland vegetation communities using a fixed-wing unmanned aerial vehicle. *International Journal of Remote Sensing*, *40*(24): pp.9103-9125.

Bhat, P.R. and Kaveriappa, K.M. 2009. Ecological studies on myristica swamp forests of Uttara Kannada, Karnataka, India. *Tropical Ecology*, 50(2): pp.329.

Bhowmik, S. 2022. Ecological and economic importance of wetlands and their vulnerability: a review. *Research Anthology on Ecosystem Conservation and Preserving Biodiversity*, http://dx.doi.org/10.4018/978-1-7998-1226-5.ch006 .

Blanckenberg, M., Mlambo, M.C., Parker, D., Motitsoe, S.N. and Reed, C. 2020. Protected and un-protected urban wetlands have similar aquatic macroinvertebrate communities: A case study from the Cape Flats Sand Fynbos region of southern Africa. *PloS one*, doi: https://doi.org/10.1371/journal.pone.0233889

Bora, M.S., Sarma, K.P. (2020). Phytoremediation of Heavy Metals/Metalloids by Native Herbaceous Macrophytes of Wetlands: Current Research and Perspectives. In: Kumar, M., Snow, D., Honda, R. (eds) Emerging Issues in the Water Environment during Anthropocene. Springer Transactions in Civil and Environmental Engineering. Springer, Singapore. https://doi.org/10.1007/978-981-32-9771-5_14

Breiman, L. 2001. Random forests. *Machine learning*, doi: https://doi.org/10.1023/A:1010933404324

Brevik, E., Pereira, P., Muñoz-Rojas, M., Miller, B., Cerda, A., Parras-Alcantara, L., Lozano-Garcia, B. Historical perspectives on soil mapping and process modelling for sustainable land use management. In press: Pereira, P., Brevik, E., Muñoz-Rojas, M., Miller, B. (eds) Soil mapping and process modelling for sustainable land use management.

Brevik, E.C., Pereira, P., Muñoz-Rojas, M., Miller, B.A., Cerdà, A., Parras-Alcántara, L. and Lozano-García, B. 2017, April. Soil mapping and process 42odelling for sustainable land use management: a brief historical review. In *EGU General Assembly Conference Abstracts*, pp. 134.

Briffa, J., Sinagra, E. and Blundell, R. 2020. Heavy metal pollution in the environment and their toxicological effects on humans. *Heliyon*, https://doi.org/10.1016/j.heliyon.2020.e04691 .

Brinson, M.M. (Ed.). 2011. Wetlands*: Integrating Multidisciplinary Concepts*. USA: Environmental & Remediation Project, PECO Energy Company

Burken, J.G., Vroblesky, D.A. and Balouet, J.C. 2011. Phytoforensics, dendrochemistry, and phytoscreening: New green tools for delineating contaminants from past and present. *Environmental Science & Technology*, *45*(15): pp.6218-6226.

Byrne, P., Reid, I. and Wood, P.J. 2013. Changes in macroinvertebrate community structure provide evidence of neutral mine drainage impacts. *Environmental Science: Processes & Impacts*, *15*(2): pp.393-404.

Canavan, K., 2016. *Investigating herbivory and plant origin on tall-statured grasses in South Africa*. Unpublished Doctoral Thesis. Grahamstown. Rhodes University.

Canavan, K., Paterson, I.D. and Hill, M.P. 2017. Exploring the origin and genetic diversity of the giant reed, Arundo donax in South Africa. *Invasive Plant Science and Management*, *10*(1): pp.53-60.

Canavan, S., Meyerson, L.A., Packer, J.G., Pyšek, P., Maurel, N., Lozano, V., Richardson, D.M., Brundu, G., Canavan, K., Cicatelli, A. and Čuda, J. 2019. Tall-statured grasses: a useful functional group for invasion science. *Biological Invasions*, *21*(1): pp.37-58.

Carlier, J., Luís, A., Alexandre, L.M. and Costa, M.C. 2020. Feasibility of co-treating olive mill wastewater and acid mine drainage. *Mine Water and the Environ*, https://doi.org/10.1007/s10230-020-00719-1

Carter, G.A. 1993. Responses of leaf spectral reflectance to plant stress. *American Journal of Botany*, *80*(3): pp.239-243.

Castaldi, P., Silvetti, M., Manzano, R., Brundu, G., Roggero, P.P. and Garau, G. 2018. Mutual effect of Phragmites australis, Arundo donax and immobilization agents on arsenic and trace metals phytostabilization in polluted soils. *Geoderma*, *https://doi.org/10.1016/j.geoderma.2017.10.040* .

Chakouri, M., Lhissou, R., El Harti, A., Maimouni, S. and Adiri, Z. 2020. Assessment of the image-based atmospheric correction of multispectral satellite images for geological mapping in arid and semi-arid regions. *Remote Sensing Applications: Society and Environment*, *https://doi.org/10.1016/j.rsase.2020.100420* .

Chaudhary, S. and McGregor, A. 2018. A critical analysis of global ecosystem services (Paristhitiki sewa) discourse in Nepal. *Land Use Policy*, *https://doi.org/10.1016/j.landusepol.2018.03.024* .

Chen, B., Teng, S., Zheng, G., Cui, L., Li, S., Staal, A., … & Xu, C. (2022). Inferring plant–plant interactions using remote sensing. Journal of Ecology, 110(10), 2268-2287. Doi: https://doi.org/10.1111/1365-2745.13980

Cho, M.A., van Aardt, J., Main, R. and Majeke, B. 2010. Evaluating variations of physiology-based hyperspectral features along a soil water gradient in a Eucalyptus grandis plantation. *International Journal of Remote Sensing*, *31*(12): pp.3143-3159.

Cicero-Fernández, D., Peña-Fernández, M., Expósito-Camargo, J. A., & Antizar-Ladislao, B. 2017. Long-term (two annual cycles) phytoremediation of heavy metal-contaminated estuarine sediments by Phragmites australis. *New biotechnology*, *doi:* https://doi.org/10.1016/j.nbt.2016.07.011

Clevers, J.G.P.W., Kooistra, L. and Salas, E.A.L. 2004. Study of heavy metal contamination in river floodplains using the red-edge position in spectroscopic data. *International Journal of Remote Sensing*, *25*(19): pp.3883-3895.

Crespo, A., Aguilar, J.M., Pintado, K. and Tinoco, B.A. 2022. Key plant species to restore plant–hummingbird pollinator communities in the southern Andes of Ecuador. *Restoration Ecology*, doi: *https://doi.org/10.1111/rec.13557* .

Cristaldi, A., Conti, G.O., Cosentino, S.L., Mauromicale, G., Copat, C., Grasso, A., Zuccarello, P., Fiore, M., Restuccia, C. and Ferrante, M. 2020. Phytoremediation potential of Arundo donax (Giant Reed) in contaminated soil by heavy metals. *Environmental Research*, doi: *https://doi.org/10.1016/j.envres.2020.109427* .

Croft, H. and Chen, J.M. (2018). Leaf Pigment Content. (Eds.)*. Comprehensive Remote Sensing,* Amsterdam. Elseivier*: pp. 117-142*

Cruzan, M. B., Weinstein, B. G., Grasty, M. R., Kohrn, B. F., Hendrickson, E. C., Arredondo, T. M., & Thompson, P. G. 2016. Small unmanned aerial vehicles (micro-UAVs, drones) in plant ecology. *Applications in plant sciences*, doi: https://doi.org/10.3732/apps.1600041

Cutler, D.R., Edwards Jr, T.C., Beard, K.H., Cutler, A., Hess, K.T., Gibson, J. and Lawler, J.J. 2007. Random forests for classification in ecology. *Ecology*, *88*(11): pp.2783-2792.

Dahlan, Mohammad, Zaini, Katsue Fukamachi, Junichi Imanishi and Shozo Shibata. 2016. Local people's knowledge of plants in kabuyutan sacred natural site in Indonesia and its implication for environmental conservation. *Nichiryoku Kogyo Journal,* 42(1): pp.32-37.

Danelli, T., Sepulcri, A., Masetti, G., Colombo, F., Sangiorgio, S., Cassani, E., Anelli, S., Adani, F. and Pilu, R. 2021. *Arundo donax L.* biomass production in a polluted area: Effects of two harvest timings on heavy metals uptake. *Applied Sciences*, *11*(3): p.1147.

Danner, M.; Locherer, M.; Hank, T.; Richter, K. 2015. Spectral Sampling with the ASD FieldSpec 4 – Theory, Measurement, Problems, Interpretation. *EnMAP Field Guides Technical Report, GFZ Data Services.* Doi: http://doi.org/10.2312/enmap.2015.008

Dar, S.A., Bhat, S.U., Rashid, I. and Dar, S.A. 2020. Current status of wetlands in Srinagar City: Threats, management strategies, and future perspectives. *Frontiers in Environmental Science*, doi: https://doi.org/10.3389/fenvs.2019.00199

Delegido, J., Verrelst, J., Meza, C.M., Rivera, J.P., Alonso, L. and Moreno, J. 2013. A red-edge spectral index for remote sensing estimation of green LAI over agroecosystems. *European Journal of Agronomy*, *46*: pp.42-52.

Delplace, G., Schreck, E., Pokrovsky, O.S., Zouiten, C., Blondet, I., Darrozes, J. and Viers, J. 2020. Accumulation of heavy metals in phytoliths from reeds growing on mining environments in Southern Europe. *Science of The Total Environment*, *doi: https://doi.org/10.1016/j.scitotenv.2019.135595* .

Deng, H. and Runger, G. 2013. Gene selection with guided regularized random forest. *Pattern Recognition*, *46*(12): pp.3483-3489.

Diaconu, M., Pavel, L.V., Hlihor, R.M., Rosca, M., Fertu, D.I., Lenz, M., Corvini, P.X. and Gavrilescu, M. 2020. Characterization of heavy metal toxicity in some plants and microorganisms—A preliminary approach for environmental bioremediation. *New Biotechnology*, *56*: pp.130-139.

Diarra, I., Kotra, K.K. and Prasad, S. 2022. Application of phytoremediation for heavy metal contaminated sites in the South Pacific: strategies, current challenges and future prospects. *Applied Spectroscopy Reviews*, *57*(6): pp.490-512.

Drusch, M., Del Bello, U., Carlier, S., Colin, O., Fernandez, V., Gascon, F., Hoersch, B., Isola, C., Laberinti, P., Martimort, P. and Meygret, A. 2012. Sentinel-2: ESA's optical high-resolution mission for GMES operational services. *Remote Sensing of Environment*, *120*: pp.25-36.

Du, B., Mao, D., Wang, Z., Qiu, Z., Yan, H., Feng, K. and Zhang, Z. 2021. Mapping wetland plant communities using unmanned aerial vehicle hyperspectral imagery by comparing object/pixel-based classifications combining multiple machine-learning algorithms. *IEEE Journal of Selected Topics in Applied Earth Observations and Remote Sensing*, *14*: pp.8249-8258.

Duffus, J. H. (2002). heavy metals" a meaningless term? *Pure Appl. Chem.*, 74: pp. 793–807.

E. Izquierdo-Verdiguier, R. Zurita-Milla and R. A. de By, "On the use of guided regularized random forests to identify crops in smallholder farm fields," *2017 9th International Workshop on the Analysis of Multitemporal Remote Sensing Images (MultiTemp)*, Brugge, Belgium, 2017, pp. 1-3,

Eid, E.M., Shaltout, K.H., Al-Sodany, Y.M., Haroun, S.A., Galal, T.M., Ayed, H., Khedher, K.M. and Jensen, K. 2021. Temporal potential of Phragmites australis as a phytoremediator to remove Ni and Pb from water and sediment in Lake Burullus, Egypt. *Bulletin of Environmental Contamination and Toxicology*, *106*: pp.516-527.

Eitel, J.U., Keefe, R.F., Long, D.S., Davis, A.S. and Vierling, L.A. 2010. Active ground optical remote sensing for improved monitoring of seedling stress in nurseries. *Sensors*, *2*(4): pp.2843-2850.

Elachi, C. and Van Zyl, J.J. 2021. *Introduction to the physics and techniques of remote sensing*, India: John Wiley & Sons.

Elnabi, A.M.K., Elkaliny, N.E., Elyazied, M.M., Azab, S.H., Elkhalifa, S.A., Elmasry, S., Mouhamed, M.S., Shalamesh, E.M., Alhorieny, N.A., Elaty, A.A.E. and Elgendy, I.M. 2023. Toxicity of heavy metals and recent advances in their removal: A review. *Toxics*, *11*(7): p.580.

Elwesemy, A. F., Elghany, N.A., Abouhadid, A., Aboelghar, M. 2020. Assessment of spectroscopic and morphological properties of some fruit crops under the influence of pollution with heavy metals using remote sensing techniques. *Arab Universities Journal of Agricultural Sciences*, doi: http://dx.doi.org/10.21608/ajs.2020.29250.1200

Farella, M., Fisher, J., Jiao, W., Key, K., & Barnes, M. (2022). Thermal remote sensing for plant ecology from leaf to globe. Journal of Ecology, 110(9): pp. 1996-2014.

Fernandes, M.R., Aguiar, F.C., Silva, J.M., Ferreira, M.T. and Pereira, J.M. 2013. Spectral discrimination of giant reed (Arundo donax L.): A seasonal study in riparian areas. *ISPRS journal of photogrammetry and Remote Sensing*, *80*: pp.80-90.

Ferner, J., Linstaedter, A., Rogass, C., Suedekum, K.H. and Schmidtlein, S. 2021. Towards Forage Resource Monitoring in subtropical Savanna Grasslands: going multispectral or hyperspectral? *European Journal of Remote Sensing*, *54*(1): pp.364-384.

Ferrario, C., Peruzzi, C., Cislaghi, A., Polesello, S., Valsecchi, S., Lava, R., Zanon, F., Santovito, G., Barausse, A. and Bonato, M. 2022. Assessment of reed grasses (Phragmites australis) performance in PFAS removal from water: a phytoremediation pilot plant study. *Water*, *14*(6): pp.946.

Filella, I. and Penuelas, J.1. 1994. The red edge position and shape as indicators of plant chlorophyll content, biomass and hydric status. *International Journal of Remote Sensing*, *15*(7): pp.1459-1470.

Flynn, K., Lee, T., Endale, D., Franzluebbers, A., Ma, S., & Zhou, Y. (2021). Assessing remote sensing vegetation index sensitivities for tall fescue (schedonorus arundinaceus) plant health with varying endophyte and fertilizer types: a case for improving poultry manuresheds. *Remote Sensing*, 13(3): pp. 521.

Frampton, W.J., Dash, J., Watmough, G. and Milton, E.J. 2013. Evaluating the capabilities of Sentinel-2 for quantitative estimation of biophysical variables in vegetation. *ISPRS Journal of Photogrammetry and Remote Sensing*, *82*: pp.83-92.

Friess, D.A., Yando, E.S., Alemu, J.B., Wong, L.W., Soto, S.D. and Bhatia, N. 2020. *Ecosystem services and disservices of mangrove forests and salt marshes*. In editors, Hawkins, S. J., Allcock, A. L., Bates, A. E., Evans, A. J., Firth, L.B., McQuaid, C. D., Russell, B. D., Smith, I. P., Swearer, S. E., Todd, P. A. (Eds.). Oceanography and marine biology. London: Taylor & Francis Group, pp. 35

Fu, P., Zhang, W., Yang, K. and Meng, F. 2020. A novel spectral analysis method for distinguishing heavy metal stress of maize due to copper and lead: RDA and EMD-PSD. *Ecotoxicology and Environmental Safety*, *doi: https://doi.org/10.1016/j.ecoenv.2020.111211*.

Fundisi, E., Tesfamichael, S., & Ahmed, F. (2022). Remote sensing of savanna woody species diversity: a systematic review of data types and assessment methods. *Plos One*, doi: https://doi.org/10.1371/journal.pone.0278529

Gallmann, J., Schüpbach, B., Jacot, K., Albrecht, M., Winizki, J., Kirchgessner, N. and Aasen, H. 2022. Flower mapping in grasslands with drones and deep learning. *Frontiers in Plant Science*, *doi: https://doi.org/10.3389/fpls.2021.774965*

Gao, Y., Zhao, Z., Shang, G., Liu, Y., Liu, S., Yan, H., Chen, Y., Zhang, X. and Li, W. 2023. Optimal feature selection and crop extraction using random forest based on GF-6 WFV data. *International Journal of Remote Sensing*, doi: https://doi.org/10.1080/01431161.2023.2216856

Gasela, M., Kganyago, M. & De Jager, G. Using resampled nSight-2 hyperspectral data and various machine learning classifiers for discriminating wetland plant species in a Ramsar Wetland site, South Africa. *Appl Geomat*, dio: https://doi.org/10.1007/s12518-024-00560-z

Genchi, G., Carocci, A., Lauria, G., Sinicropi, M.S. and Catalano, A. 2020. Nickel: Human health and environmental toxicology. *International Journal of Environmental Research and Public Health*, *17*(3): pp.679.

Genchi, G., Sinicropi, M.S., Lauria, G., Carocci, A. and Catalano, A. 2020. The effects of cadmium toxicity. *International Journal of Environmental Research and Public Health*, *17*(11): pp.3782.

Gerhards, M., Schlerf, M., Mallick, K. and Udelhoven, T. 2019. Challenges and future perspectives of multi-/Hyperspectral thermal infrared remote sensing for crop water-stress detection: A review. *Remote Sensing*, *11*(10): pp.1240.

Ghori, N.H., Ghori, T., Hayat, M.Q., Imadi, S.R., Gul, A., Altay, V. and Ozturk, M. 2019. Heavy metal stress and responses in plants. *International Journal of Environmental Science and Technology*, *16*: pp.1807-1828.

Golubkov, G.V., Manzhelii, M.I., Berlin, A.A., Eppelbaum, L.V., Lushnikov, A.A., Morozov, I.I., Dmitriev, A.V., Adamson, S.O., Dyakov, Y.A., Morozov, A.N. and Golubkov, M.G. 2020. The problems of passive remote sensing of the earth's surface in the range of 1.2–1.6 ghz. *Atmosphere*, *11*(6): p.650.

Goolsby, J.A., Moran, P., Maricela Martínez Jiménez, Yang, C., Canavan, K., Paynter, Q., Ota, N. and Kriticos, D.J. 2023. Biology of Invasive Plants 4. *Arundo donax* L.. *Invasive Plant Science and Management*, 16(2): pp.81–109.

Gordon-Gray, K.D., Baijnath, H., Ward, C.J. and Wragg, P.D. 2009. Studies in Cyperaceae in southern Africa 42: Pseudo-vivipary in South African Cyperaceae. *South African Journal of Botany*, *75*(1): pp.165-171.

Govender, M., Govender, P.J., Weiersbye, I.M., Witkowski, E.T.F. and Ahmed, F. 2009. Review of commonly used remote sensing and ground-based technologies to measure plant water stress. *Water SA*, *doi: https://doi.org/10.4314/wsa.v35i5.49201*

Goyal, D., Yadav, A., Prasad, M., Singh, T.B., Shrivastav, P., Ali, A., Dantu, P.K. and Mishra, S. 2020: Effect of Heavy Metals on Plant Growth: An Overview. In: Naeem, M., Ansari, A., Gill, S. (eds.). *Contaminants in Agriculture*. Switzerland: Springer, pp. 79-101.

Goyens, C., Marty, S., Leymarie, É., Antoine, D., Babin, M., & Bélanger, S. (2018). High angular resolution measurements of the anisotropy of reflectance of sea ice and snow. *Earth and Space Science*, 5(1): pp. 30-47.

Guarino, F., Miranda, A., Castiglione, S. and Cicatelli, A. 2020. Arsenic phytovolatilization and epigenetic modifications in Arundo donax L. assisted by a PGPR consortium. *Chemosphere*, *doi: https://doi.org/10.1016/j.chemosphere.2020.126310* .

Guimond, J. and Tamborski, J. 2021. Salt marsh hydrogeology: A review. Water, 13(4): pp.543.

Guo, L., Ott, D.W. and Cutright, T.J. 2014. Accumulation and histological location of heavy metals in *Phragmites australis* grown in acid mine drainage contaminated soil with or without citric acid. *Environmental and Experimental Botany*, *105*: pp.46-54.

Guo, Q., Su, Y. and Hu, T. 2023. *LiDAR principles, processing and applications in forest ecology*. China: Academic Press.

Guthrie, G. 2007: *Impacts of the invasive reed Arundo donax on biodiversity at the community-ecosystem level*. Unpublished Doctoral dissertation. Cape Town: University of the Western Cape.

Guzzi, G., Ronchi, A. and Pigatto, P. 2021. Toxic effects of mercury in humans and mammals. *Chemosphere*, doi: *https://doi.org/10.1016/j.chemosphere.2020.127990* .

Hachicho, Z. 2023: *The definition of fens and bogs: An international meta-study*. Unpublished Dissertation. Uppsala: Uppsala University.

Hannula, H., Heinilä, K., Böttcher, K., Mattila, O., Salminen, M., & Pulliainen, J. (2020). Laboratory, field, mast-borne and airborne spectral reflectance measurements of boreal landscape during spring. *Earth System Science Data,* 12(1): 719-740.

Harmse, J.T. and Le Grange, C.N. 1994. The influence of urbanization on pans on the East Rand (Johannesburg, South Africa). *Landscape and urban planning*, *28*(2-3): pp.217-224.

Hasan, S.M.M., Akber, M.A., Bahar, M.M., Islam, M.A., Akbor, M.A., Siddique, M.A.B. and Islam, M.A. 2021. Chromium contamination from tanning industries and Phytoremediation potential of native plants: A study of savar tannery industrial estate in Dhaka, Bangladesh. *Bulletin of Environmental Contamination and Toxicology*, *106*(6): pp.1024-1032.

Hassani, K., Gholizadeh, H., Taghvaeian, S., Natalie, V., Carpenter, J. and Jacob, J. 2023. Assessing the impact of spatial resolution of UAS-based remote sensing and spectral resolution of proximal sensing on crop nitrogen retrieval accuracy. *International Journal of Remote Sensing*, *44*(14): pp.4441-4464.

He, L., Wang, S., Liu, M., Chen, Z., Xu, J. and Dong, Y. 2023. Transport and transformation of atmospheric metals in ecosystems: A review. *Journal of Hazardous Materials Advances*, *https://doi.org/10.1016/j.hazadv.2022.100218* .

Holzman, M.E., Rivas, R.E. and Bayala, M.I. 2021. Relationship between TIR and NIR-SWIR as indicator of vegetation water availability. *Remote Sensing*, *13*(17): pp.3371.

Homolová, L., Malenovský, Z., Clevers, J., García-Santos, G., & Schaepman, M. 2013. Review of optical-based remote sensing for plant trait mapping. *Ecological Complexity*, doi: https://doi.org/10.1016/j.ecocom.2013.06.003

Homolová, L., Malenovský, Z., Clevers, J.G., García-Santos, G. and Schaepman, M.E. 2013. Review of optical-based remote sensing for plant trait mapping. *Ecological Complexity*, *15*, pp.1-16.

Hong, Z., Zhao, Q., Chang, J., Peng, L., Wang, S., Hong, Y., Liu, G. and Ding, S. 2020. Evaluation of water quality and heavy metals in wetlands along the Yellow River in Henan Province. *Sustainability*, *12*(4), p.1300.

Howard-Williams, C. and Gaudet, J.J. 1985. The structure and functioning of African swamps. In The ecology and management of African wetland vegetation: A botanical account of African swamps and shallow waterbodies Dordrecht. Netherlands: Springer, pp. 153-175.

Huang, P., Luo, X., Jin, J., Wang, L., Zhang, L., Liu, J. and Zhang, Z. 2018. Improving high-throughput phenotyping using fusion of close-range hyperspectral camera and low-cost depth sensor. *Sensors*, *18*(8): pp.2711.

Inoue, Y. 2020. Satellite-and drone-based remote sensing of crops and soils for smart farming–a review. *Soil Science and Plant Nutrition*, *66*(6): pp.798-810.

Iqbal, I.M., Balzter, H. and Shabbir, A. 2021. Identifying the Spectral Signatures of Invasive and Native Plant Species in Two Protected Areas of Pakistan through Field Spectroscopy. *Remote Sensing*, *https://doi.org/10.3390/rs13194009* .

Izquierdo-Verdiguier, E., Zurita-Milla, R. and de By, R.A. 2017. On the use of guided regularized random forests to identify crops in smallholder farm fields. In *2017 9th International Workshop on the Analysis of Multitemporal Remote Sensing Images (MultiTemp)* (pp. 1-3). IEEE.

Jacklin, D. M., Brink, I., & Jacobs, S. M. 2021. Efficiencies of indigenous South African plant biofilters for urban stormwater runoff water quality improvement with a focus on nutrients and metals. *Journal of Water Supply: Research and Technology-Aqua*, 70(7): pp. 1094-1110

Jaishankar, M., Tseten, T., Anbalagan, N., Mathew, B.B. and Beeregowda, K.N. 2014. Toxicity, mechanism and health effects of some heavy metals. *Interdisciplinary toxicology*, *7*(2): pp.60.

Kafle, A., Timilsina, A., Gautam, A., Adhikari, K., Bhattarai, A. and Aryal, N. 2022. Phytoremediation: Mechanisms, plant selection and enhancement by natural and synthetic agents. *Environmental Advances*, https://doi.org/10.1016/j.envadv.2022.100203

Kaur, H. and Garg, N. 2021. Zinc toxicity in plants: A review. *Planta*, *253*(6), p.129.

Keeran, N.S., Usha, B. and Ganesan, G. 2021. P-type ATPases and their role in metal homeostasis in plants. In *Metal and Nutrient Transporters in Abiotic Stress*, https://doi.org/10.1016/B978-0-12-817955-0.00002-8 .

Kibra, M.G. 2008. Effects of mercury on some growth parameters of rice (Oryza sativa L.). *Soil Environ*, *27*(1), pp.23-28.

Kim, Y., Choi, J., Han, D. and Kim, Y. 2015. Block-based fusion algorithm with simulated band generation for hyperspectral and multispectral images of partially different wavelength ranges. *IEEE Journal of Selected Topics in Applied Earth Observations and Remote Sensing*, *8*(6), pp.2997-3007.

Kingsford, R. T., Basset, A., & Jackson, L. J. 2016. Wetlands: conservation's poor cousins. Aquatic Conservation: Marine and Freshwater Ecosystems, 26(5): pp. 892-916.

Kior, A., Sukhov, V. and Sukhova, E. 2021, December. Application of reflectance indices for remote sensing of plants and revealing actions of stressors. In *Photonics*, doi: https://doi.org/10.3390/photonics8120582

Knox, A. K., Dahlgren, R. A., Tate, K. W., & Atwill, E. R. 2008. Efficacy of natural wetlands to retain nutrient, sediment and microbial pollutants. *Journal of Environmental Quality*, 37(5): pp. 1837-1846.

Konietschke, F., Schwab, K. and Pauly, M. 2021. Small sample sizes: A big data problem in high-dimensional data analysis. *Statistical Methods in Medical Research*, *30*(3): pp.687-701.

Kumar, A., Aery, N.C. (Eds.). 2016: Impact, Metabolism, and Toxicity of Heavy Metals in Plants. In Singh, A., Prasad, S., Singh, R. *Plant Responses to Xenobiotics*. Doi: https://doi.org/10.1007/978-981-10-2860-1_7

Kumar, V., Pandita, S., Sidhu, G.P.S., Sharma, A., Khanna, K., Kaur, P., Bali, A.S. and Setia, R., 2021. Copper bioavailability, uptake, toxicity and tolerance in plants: A comprehensive review. *Chemosphere*, *262*, p.127810.

Kumar, V., Shah, M.P. and Shahi, S.K. (Eds.). 2022. *Phytoremediation technology for the removal of heavy metals and other contaminants from soil and water*. India: Elsevier.

Kumari, R., Shukla, S.K., Parmar, K., Bordoloi, N., Kumar, A., Saikia, P. 2020: Wetlands Conservation and Restoration for Ecosystem Services and Halt Biodiversity Loss: An Indian Perspective. In: Upadhyay, A., Singh, R., Singh, D. *Restoration of Wetland Ecosystem: A Trajectory Towards a Sustainable Environment*. Doi: https://doi.org/10.1007/978-981-13-7665-8_6

Kvíčala, M., Lacková, E. and Štamborská, M. 2013. Internal Reflectance Modelling of Hordeum vulgare Leaves During Drying. *Journal of Chemistry*, *doi: https://doi.org/10.1155/2013/210679* .

Lešková, A., Zvarík, M., Araya, T. and Giehl, R.F. 2020. Nickel toxicity targets cell wall-related processes and PIN2-mediated auxin transport to inhibit root elongation and gravitropic responses in Arabidopsis. *Plant and Cell Physiology*, *61*(3), pp.519-535.

Leuning, R., Hughes, D., Daniel, P., Coops, N.C. and Newnham, G. 2006. A multi-angle spectrometer for automatic measurement of plant canopy reflectance spectra. *Remote Sensing of Environment*, *103*(3), pp.236-245.

Li, C., Czyż, E.A., Halitschke, R., Baldwin, I.T., Schaepman, M.E. and Schuman, M.C. 2023. Evaluating potential of leaf reflectance spectra to monitor plant genetic variation. *Plant Methods*, *19*(1), p.108.

Li, W., Cui, L., Sun, B., Zhao, X., Gao, C., Zhang, Y., Zhang, M., Pan, X., Lei, Y. and Ma, W. 2017. Distribution patterns of plant communities and their associations with environmental soil factors on the eastern shore of Lake Taihu, China. *Ecosystem Health and Sustainability*, doi: *https://doi.org/10.1080/20964129.2017.1385004* .

Li, W., Sun, Z., Lu, S. and Omasa, K. 2019. Estimation of the leaf chlorophyll content using multiangular spectral reflectance factor. *Plant, Cell & Environment*, *42*(11), pp.3152-3165.

Li, Y., Feng, Y., Wang, X.Y., Liu, B. and Lv, G.H. 2014. Failure of DNA barcoding in discriminating Calligonum species. *Nordic Journal of Botany*, *32*(4), pp.511-517.

Li, Z., Xu, D. and Guo, X. 2014. Remote sensing of ecosystem health: opportunities, challenges, and future perspectives. *Sensors*, doi: *https://doi.org/10.3390/s141121117* .

Liaghat, S., Mansor, S., Ehsani, R., Shafri, H.Z.M., Meon, S. and Sankaran, S. 2014. Mid-infrared spectroscopy for early detection of basal stem rot disease in oil palm. *Computers and electronics in agriculture*, *doi: https://doi.org/10.1016/j.compag.2013.12.012*

Liang, S. (Ed.). 2017. *Comprehensive remote sensing*. United States: Elsevier.

Lino, G., Espigul, P., Nogués, S. and Serrat, X. 2023. Arundo donax L. growth potential under different abiotic stress. *Heliyon*, doi: https://doi.org/10.1016/j.heliyon.2023.e15521

Lisviananda, N., Sugianto, S., & Rusdi, M. 2022. Rice growth phase analysis in pidie regency, Indonesia using multitemporal sentinel-2 image data: a spectral angle mapper approach. *IOP Conference Series: Earth and Environmental Science*, doi: 012068. https://doi.org/10.1088/1755-1315/951/1/012068

Liu, Y., Li, W., Wu, G. and Xu, X. 2011. Feasibility of estimating heavy metal contaminations in floodplain soils using laboratory-based hyperspectral data—A case study along Le'an River, China. *Geo-spatial Information Science*, *14*(1), pp.10-16.

Luan, J., Zhang, C., Xu, B., Xue, Y. and Ren, Y. 2020. The predictive performances of random forest models with limited sample size and different species traits. *Fisheries Research*, *https://doi.org/10.1016/j.fishres.2020.105534* .

Mabhungu, L., Adam, E. and Newete, S.W. 2019. Monitoring of phytoremediating wetland macrophytes using remote sensing: the case of common reed (*Phragmites australis* (Cav.) Trin. Ex Steud.) and the giant reed (Arundo donax L.). A review. *Applied Ecology & Environmental Research*, *available at: https://aloki.hu/pdf/1704_79577972.pdf* [Accessed on 20 October 2023).

Madani, A.A. 2011. Spectral properties of carbonatized ultramafic mantle xenoliths and their host olivine basalts, Jabal Al Maqtal basin, South Eastern Desert, Egypt, using ASD FieldSpec spectroradiometer. *The Egyptian Journal of Remote Sensing and Space Science*, *14*(1), pp.41-48.

Magney, T.S., Bowling, D.R., Logan, B.A., Grossmann, K., Stutz, J., Blanken, P.D., Burns, S.P., Cheng, R., Garcia, M.A., Köhler, P. and Lopez, S. 2019. Mechanistic evidence for tracking the seasonality of photosynthesis with solar-induced fluorescence. *Proceedings of the National Academy of Sciences*, *doi: https://doi.org/10.1073/pnas.1900278116*

Mahlein, A.K., Hammersley, S., Oerke, E.C., Dehne, H.W., Goldbach, H. and Grieve, B. 2015. Supplemental blue LED lighting array to improve the signal quality in hyperspectral imaging of plants. *Sensors*, *doi: https://doi.org/10.3390/s150612834* .

Maia, K.P., Vaughan, I.P. and Memmott, J. 2019. Plant species roles in pollination networks: an experimental approach. *Oikos*, *128*(10), pp.1446-1457.

Malapane, C. 2021: *Mapping the distribution and abundance of common needs Phragmites australis in the Nylsvley Wetland, South Africa using SPOT and Landsat imagery*. Unpublished Doctoral dissertation. Venda: University of Venda.

Manevski, K., Manakos, I., Petropoulos, G.P. and Kalaitzidis, C. 2011. Discrimination of common Mediterranean plant species using field spectroradiometry. *International Journal of Applied Earth Observation and Geoinformation*, *13*(6), pp.922-933.

Manolakis, D. and Shaw, G. 2002. Detection algorithms for hyperspectral imaging applications. *IEEE signal processing magazine*, *19*(1), pp.29-43.

Mansour, K., Mutanga, O., Everson, T. and Adam, E. 2012. Discriminating indicator grass species for rangeland degradation assessment using hyperspectral data resampled to AISA Eagle resolution. *ISPRS Journal of Photogrammetry and Remote Sensing*, *70*, pp.56-65.

Masindi, V. and Muedi, K.L. 2018. Environmental contamination by heavy metals. *Heavy metals*, *10*, pp.115-132.

Meroni, M., Barducci, A., Cogliati, S., Castagnoli, F., Rossini, M., Busetto, L., Migliavacca, M., Cremonese, E., Galvagno, M., Colombo, R. and Di Cella, U.M. 2011. The hyperspectral irradiometer, a new instrument for long-term and unattended field spectroscopy measurements. *Review of Scientific Instruments*, doi: https://doi.org/10.1063/1.3574360 .

Mganga, N., Manoko, M.L.K. and Rulangaranga, Z.K. 2011. Classification of plants according to their heavy metal content around North Mara gold mine, Tanzania: implication for phytoremediation. *Tanzania journal of science*, available at: https://www.ajol.info/index.php/tjs/article/view/73619 [Accessed 26 August 2024].

Milke, J., Gałczyńska, M. and Wróbel, J. 2020. The importance of biological and ecological properties of *Phragmites australis* (Cav.) Trin. Ex Steud., in phytoremendiation of aquatic ecosystems—the review. *Water*, *12*(6), p.1770.

Mir, A.R., Pichtel, J. and Hayat, S. 2021. Copper: uptake, toxicity and tolerance in plants and management of Cu-contaminated soil. *Biometals*, *34*(4): pp.737-759.

Mirzaei, M., Marofi, S., Abbasi, M., Solgi, E., Karimi, R. and Verrelst, J., 2019. Scenario-based discrimination of common grapevine varieties using in-field hyperspectral data in the western of Iran. *International Journal of Applied Earth Observation and Geoinformation*, *80*: pp.26-37.

Misra, S., Li, H. and He, J. 2020. Noninvasive fracture characterization based on the classification of sonic wave travel times. *Machine learning for subsurface characterization*, *4*: pp.243-287.

Mitra, S., Chakraborty, A.J., Tareq, A.M., Emran, T.B., Nainu, F., Khusro, A., Idris, A.M., Khandaker, M.U., Osman, H., Alhumaydhi, F.A. and Simal-Gandara, J. 2022. Impact of heavy metals on the environment and human health: Novel therapeutic insights to counter the toxicity. *Journal of King Saud University-Science*, doi: https://doi.org/10.1016/j.jksus.2022.101865

Mitsch, W.J. and Gosselink, J.G. 2015. Wetlands. United States: *John Wiley & Sons.*

Möckel, T., Dalmayne, J., Schmid, B., Prentice, H., & Hall, K. 2016. Airborne hyperspectral data predict fine-scale plant species diversity in grazed dry grasslands. *Remote Sensing*, 8(2), doi: https://doi.org/10.3390/rs8020133

Mok, W.J., Ghaffar, M.A., Noor, M.I.M., Lananan, F. and Azra, M.N. 2023. Understanding climate change and heavy metals in coastal areas: a macroanalysis assessment. *Water*, *doi: https://doi.org/10.3390/w15050891*

Moreau, J. W., Fournelle, J., & Banfield, J. F. 2013. Quantifying heavy metals sequestration by sulfate-reducing bacteria in an acid mine drainage-contaminated natural wetland. *Frontiers in Microbiology*, doi: https://doi.org/10.3389/fmicb.2013.00043

Morsy, M., Nossier, M., Elsebaay, A.E. and Abd-Elrahman, S. 2022. Phytoremediation of Pb and Cd by Alfalfa (Medicago sativa L.): An Applied Study in the Presence of Lettuce Plants (Lactuca sativa L.). *Arab Universities Journal of Agricultural Sciences*, *30*(1), pp.163-174.

Müllerová, J., Pergl, J. and Pyšek, P., 2013. Remote sensing as a tool for monitoring plant invasions: Testing the effects of data resolution and image classification approach on the detection of a model plant species Heracleum mantegazzianum (giant hogweed). *International Journal of Applied Earth Observation and Geoinformation*, *25*, pp.55-65.

Muñoz-Huerta, R. F., Guevara-González, R. G., Contreras-Medina, L. M., Torres-Pacheco, I., Prado-Olivarez, J., & Ocampo-Velázquez, R. V. 2013. A review of methods for sensing the nitrogen status in plants: advantages, disadvantages and recent advances. *Sensors*, doi: 10823-10843. https://doi.org/10.3390/s130810823

Munyati, C., Balzter, H. and Economon, E. 2020. Correlating Sentinel-2 MSI-derived vegetation indices with in-situ reflectance and tissue macronutrients in savannah grass. *International Journal of Remote Sensing*, doi: https://doi.org/10.1080/01431161.2019.1708505 .

Mureriwa, N., Adam, E., Sahu, A. and Tesfamichael, S. 2016. Examining the spectral separability of Prosopis glandulosa from co-existent species using field spectral measurement and guided regularized random forest. *Remote Sensing*, *8*(2): p.144.

Musabyimana, J. P. and Bazimenyera, J. d. D. 2023. Assessment of the impacts of converting natural wetlands to agricultural farms. Case of nyabugogo, Kigali city, Rwanda. *Agricultural Sciences*, doi: https://doi.org/10.4236/as.2023.143027

Mustamu, N.E., Victor, M.M. and Sihombing, V. 2021. Drone simulation for agriculture and LoRa based approach. *Internet of Things and Artificial Intelligence Journal*, *1*(4), pp.221-235.

Nagasubramanian, K., Jones, S., Singh, A.K., Sarkar, S., Singh, A. and Ganapathysubramanian, B. 2019. Plant disease identification using explainable 3D deep learning on hyperspectral images. *Plant Methods*, *15*, pp.1-10.

Nasir, M., Nur, M., Pandiangan, D., Mambu, S.M., Fauziah, S., Raya, I., Fudholi, A. and Irfandi, R. 2022. Phytoremediation study of water hyacinth (Eichhornia crassipes) on zinc metal ion (Zn2+). *International Journal of Design & Nature and Ecodynamics*, *17*(3), pp.417-422.

Nedjimi, B. 2021. Phytoremediation: a sustainable environmental technology for heavy metals decontamination. *SN Applied Sciences*, *3*(3), p.286.

Newete, S.W. and Byrne, M.J. 2016. The capacity of aquatic macrophytes for phytoremediation and their disposal with specific reference to water hyacinth. *Environmental Science and Pollution Research*, *doi: https://doi.org/10.1007/s11356-016-6329-6*

Nguegang, B., Masindi, V., Msagati, T.A.M. and Tekere, M. 2021. The treatment of acid mine drainage using vertically flowing wetland: Insights into the fate of chemical species. *Minerals*, doi: https://doi.org/10.3390/min11050477 .

Nidamanuri, R.R. 2020. Hyperspectral discrimination of tea plant varieties using machine learning, and spectral matching methods. *Remote Sensing Applications: Society and Environment*, doi: https://doi.org/10.1016/j.rsase.2020.100350 .

Niu, Y., Chen, F., Li, Y. and Ren, B. 2021. Trends and sources of heavy metal pollution in global river and lake sediments from 1970 to 2018. *Reviews of Environmental Contamination and Toxicology, 257*, pp.1-35.

Niyogi, D.K., Lewis Jr, W.M. and McKnight, D.M. 2001. Litter breakdown in mountain streams affected by mine drainage: biotic mediation of abiotic controls. *Ecological applications*, *11*(2), pp.506-516.

Noomen, M., Hakkarainen, A., van der Meijde, M. and van der Werff, H. 2015. Evaluating the feasibility of multitemporal hyperspectral remote sensing for monitoring bioremediation. *International Journal of Applied Earth Observation and Geoinformation*, *34*, pp.217-225.

Nriagu, J.O. 1989. A global assessment of natural sources of atmospheric trace metals. *Nature*, *338* (6210), pp.47-49.

Obeidat, W., Avila, L., Earl, H. and Lukens, L. 2018. Leaf spectral reflectance of maize seedlings and its relationship to cold tolerance. *Crop Science*, doi: http://dx.doi.org/10.2135/cropsci2018.02.0115 .

Octavia, M. T. and Supriatna, S. (2022). Rice plant health spatial study with sentinel and spot imagery in parakansalak district. IOP Conference Series: Earth and Environmental Science, doi: 10.1088/1755-1315/1111/1/012023

Oda, Y.S., de Oliveira, L.O., De Paula, S., de Oliveira, A.O. and de Castro Neto, J.C. 2023. Weed detection among soybean plants in artificial lighting environment using multispectral images and computer vision. In *SPIE-CLP Conference on Advanced Photonics 2023*, doi: http://dx.doi.org/10.1117/12.2686194 .

Odindi, J., Adam, E., Abdel-Rahman, E.M. and Mutanga, O. 2018. Testing the spectral resolutions of the new multispectral sensors for detecting Phaeosphaeria leaf spot (PLS) infestations in maize crop. *South African Journal of Geomatics*, *7*(1), pp.1-10.

OLLENDORF, A.L., Mulholland, S.C. and Rapp Jr, G. 1988. Phytolith analysis as a means of plant identification: Arundo donax and Phragmites communis. *Annals of Botany*, *61*(2), pp.209-214.

Omasa, K., Ono, E., Ishigami, Y., Shimizu, Y., & Araki, Y. 2022. Plant functional remote sensing and smart farming applications. *International Journal of Agricultural and Biological Engineering,* 15(4), 1-6.

Onojeghuo, A.O. and Blackburn, G.A. 2011. Mapping reedbed habitats using texture-based classification of QuickBird imagery. *International Journal of Remote Sensing*, *doi: https://doi.org/10.1080/01431161.2010.532822* .

Orimoloye, I.R., Kalumba, A.M., Mazinyo, S.P. and Nel, W. 2020. Geospatial analysis of wetland dynamics: Wetland depletion and biodiversity conservation of Isimangaliso Wetland, South Africa. *Journal of King Saud University-Science*, *32*(1): pp.90-96.

Osco, L. P., Ramos, A. P. M., Moriya, É. A. S., Bavaresco, L. G., Lima, B. C. d., Estrabis, N. V., … & Araújo, F. F. d. 2019. Modeling hyperspectral response of water-stress induced lettuce plants using artificial neural networks. *Remote Sensing*, doi: https://doi.org/10.3390/rs11232797

Pan, Y., Cieraad, E., Armstrong, J., Armstrong, W., Clarkson, B. R., Colmer, T. D., … & Bodegom, P. M. v. 2020. Global patterns of the leaf economics spectrum in wetlands. *Nature Communications*, doi: https://doi.org/10.1038/s41467-020-18354-3

Pandey, P., Shah, D.N. and Tachamo-Shah, R.D. 2020. Impact of invasive alien plant species on aquatic biodiversity of Koshi Tappu Wetlands: Ramsar Site, Nepal. *Banko Janakari*, *30*(2): pp.48-58.

Pandita, D. and Pamuru, R.R. 2022. Genomic approaches for phytoremediation of trace and hazardous metals. In *Hazardous and Trace Materials in Soil and Plants*, https://doi.org/10.1016/B978-0-323-91632-5.00022-7

Papazoglou, E.G. and Bouranis, D.L. 2005. physiological responses of arundo donax l. Exposed to heavy metals. Available at:

https://www.researchgate.net/publication/335381089_PHYSIOLOGICAL_RESPONSES_OF_ARUNDO_DONAX_L_EXPOSED_TO_HEAVY_METALS [Accessed on 25 August 2024].

Peddle, D.R., White, H.P., Soffer, R.J., Miller, J.R. and Ledrew, E.F. 2001. Reflectance processing of remote sensing spectroradiometer data. *Computers & geosciences*, doi: https://doi.org/10.1016/S0098-3004(00)00096-0 .

Pegg, J., South, J., Hill, J.E., Durland-Donahou, A. and Weyl, O.L. 2022. Impacts of alien invasive species on large wetlands. *In Fundamentals of Tropical Freshwater Wetlands*. Available from: https://www.sciencedirect.com/science/article/abs/pii/B9780128223628000189#:~:text=The%20alien%20taxon%20is%20toxic,inhalation%2C%20or%20contact%20to%20wildlife.&text=Grazing%2C%20herbivory%2C%20or%20browsing%20by%20the%20alien%20taxon.&text=The%20alien%20taxon%20causes%20changes,and%2For%20water%20cycling). [Accessed 25 August 2024].

Peng, H., Kroneck, P.M. and Küpper, H. 2013. Toxicity and deficiency of copper in Elsholtzia splendens affect photosynthesis biophysics, pigments and metal accumulation. *Environmental Science & Technology*, *doi: https://doi.org/10.1021/es3050746* .

Pérez-Sirvent, C., Hernández-Pérez, C., Martínez-Sánchez, M.J., García-Lorenzo, M.L. and Bech, J. 2017. Metal uptake by wetland plants: implications for phytoremediation and restoration. *Journal of Soils and Sediments*, doi: https://doi.org/10.1016/j.envint.2003.11.002 .

Plaza, A., Benediktsson, J.A., Boardman, J.W., Brazile, J., Bruzzone, L., Camps-Valls, G., Chanussot, J., Fauvel, M., Gamba, P., Gualtieri, A. and Marconcini, M. 2009. Recent advances in techniques for hyperspectral image processing. *Remote Sensing of Environment*, doi: https://doi.org/10.1016/j.rse.2007.07.028 .

Poças, I., Cunha, M. and Pereira, L.S. 2012. Dynamics of mountain semi-natural grassland meadows inferred from SPOT-VEGETATION and field spectroradiometer data. *International Journal of Remote Sensing*, doi: https://doi.org/10.1080/01431161.2011.645084 .

Ponce-Fontenla, S., Serrano, M., Carballal, R., & Regos, A. 2021. Sentinel 2 images enable reliable prediction of fine-scale habitat dynamics of narrow endemic plant species in serpentine soils. *Applied Vegetation Science,* doi: https://doi.org/10.1111/avsc.12614

Pourret, O. 2018. On the necessity of banning the term “heavy metal” from the scientific literature. *Sustainability*, doi: https://doi.org/10.3390/su10082879

Pradhan, S., Sehgal, V.K., Bandyopadhyay, K.K., Sahoo, R.N., Panigrahi, P., Parihar, C.M. and Jat, S.L. 2018. Comparison of vegetation indices from two ground based sensors. *Journal of the Indian Society of Remote Sensing*, doi: https://doi.org/10.1007/s12524-017-0671-0 .

Prasad, M.N.V. ed., 2018. *Transgenic plant technology for remediation of toxic metals and metalloids*. Doi: https://doi.org/10.1016/C2017-0-01241-7

Prasad, R. ed. 2021: *Phytoremediation for environmental sustainability*. Singapore: Springer.

Psomas, A., Kneubühler, M., Huber, S., Itten, K. and Zimmermann, N.E. 2011. Hyperspectral remote sensing for estimating aboveground biomass and for exploring species richness patterns of grassland habitats. *International Journal of Remote Sensing*, doi: https://doi.org/10.1080/01431161.2010.532172 .

Qu, R., Han, G., Liu, M. and Li, X. 2019. The mercury behavior and contamination in soil profiles in mun river basin, Northeast Thailand. *International Journal of Environmental Research and Public Health*, doi: https://doi.org/10.3390%2Fijerph16214131 .

Rai, P.K. 2019. Heavy metals/metalloids remediation from wastewater using free floating macrophytes of a natural wetland. *Environmental Technology & Innovation*, doi: https://doi.org/10.1016/j.eti.2019.100393 .

Rai, P.K. and Singh, J.S. 2020. Invasive alien plant species: Their impact on environment, ecosystem services and human health. *Ecological Indicators*, *doi: https://doi.org/10.1016/j.ecolind.2019.106020* .

Ramachandiran, K., Pazhanivelan, S., Amanullah, M., Geethalakshmi, V., Sivasamy, R., & Raja, N. 2016. Quantifying the nitrogen and water stress of maize using spectral vegetation indices. *International Journal of Bio-Resource and Stress Management,* doi: https://doi.org/10.23910/ijbsm/2016.7.1.1367a

Ramsar, I. 1971. Convention on wetlands of international importance, especially as waterfowl habitat. *Ramsar (Iran),* 2. Available at: https://www.unesco.org/en/biodiversity/wetlands . [Accessed on 15 February 2024].

Ranganathan, P., Ravikanth, G. and Aravind, N.A. 2022. A review of research and conservation of Myristica swamps, a threatened freshwater swamp of the Western Ghats, India. *Wetlands Ecology and Management*, doi: https://doi.org/10.1007/s11273-021-09825-5 .

Rani, A., Kumar, A., Lal, A., & Pant, M. 2013. Cellular mechanisms of cadmium-induced toxicity: a review. *International Journal of Environmental Health Research*, doi: https://doi.org/10.1080/09603123.2013.835032

Rascio, N. and Navari-Izzo, F. 2011. Heavy metal hyperaccumulating plants: how and why do they do it? And what makes them so interesting? *Plant Science*, doi: https://doi.org/10.1016/j.plantsci.2010.08.016 .

Raypah, M.E., Imran Mohd Nasru, M., Hazeem Hasnol Nazim, M., Omar, A.F., Muncan, J., Muhammad Zahir, S.A.D., Jamlos, M.F. and Mahmod Jasim, H. 2024. Reflectance spectra for identifying stress in different parts of leaf: a case study on oil palm seedlings. *International Journal of Remote Sensing*, *45*(3): pp.954-980.

Rebelo, L., McCartney, M., & Finlayson, C. M. (2009). Wetlands of sub-saharan 57odell: distribution and contribution of agriculture to livelihoods. *Wetlands Ecology and Management*, 18(5), 557-572. https://doi.org/10.1007/s11273-009-9142-x

Rehman, A.U., Nazir, S., Irshad, R., Tahir, K., ur Rehman, K., Islam, R.U. and Wahab, Z. 2021. Toxicity of heavy metals in plants and animals and their uptake by magnetic iron oxide nanoparticles. *Journal of Molecular Liquids*, doi: https://doi.org/10.1016/j.molliq.2020.114455 .

Rezania, S., Park, J., Rupani, P.F., Darajeh, N., Xu, X. and Shahrokhishahraki, R. 2019. Phytoremediation potential and control of *Phragmites australis*as a green phytomass: An overview. *Environmental Science and Pollution Research*, *26*: pp.7428-7441.

Riato, L., Leira, M., Bella, V. D., & Oberholster, P. J. 2018. Development of a diatom-based multimetric index for acid mine drainage impacted depressional wetlands. *Science of the Total Environment*, 612: pp. 214-222.

Rock, B.N., Hoshizaki, T. and Miller, J.R. 1988. Comparison of in situ and airborne spectral measurements of the blue shift associated with forest decline. *Remote Sensing of Environment*, *24*(1): pp.109-127.

Roman, A. and Ursu, T. 2016. Multispectral satellite imagery and airborne laser scanning techniques for the detection of archaeological vegetation marks. *Landscape archaeology on the northern frontier of the roman empire at porolissum: an interdisciplinary research project. Cluj-Napoca: Mega Publishing House*, available at:
https://www.researchgate.net/publication/315797574_Multispectral_satellite_imagery_and_airborne_laser_scanning_techniques_for_the_detection_of_archaeological_vegetation_marks .[Accessed on 20 September 2023]

Rouse, J.H., Shaw, J.A., Lawrence, R.L., Lewicki, J.L., Dobeck, L.M., Repasky, K.S. and Spangler, L.H. 2010. Multi-spectral imaging of vegetation for detecting CO 2 leaking from underground. *Environmental Earth Sciences*, *60*: pp.313-323.

Sabins Jr, F.F. and Ellis, J.M. 2020. *Remote sensing: Principles, interpretation, and applications*. United States: Waveland Press.

Sagan, V., Maimaitijiang, M., Bhadra, S., Maimaitiyiming, M., Brown, D.R., Sidike, P. and Fritschi, F.B. 2021. Field-scale crop yield prediction using multi-temporal WorldView-3 and PlanetScope satellite data and deep learning. *ISPRS Journal of Photogrammetry and Remote Sensing*, *174*: pp.265-281.

Saha, A., Sen Gupta, B., Patidar, S. and Martínez-Villegas, N. 2022. Identification of soil arsenic contamination in rice paddy field based on hyperspectral reflectance approach. *Soil Systems*, *6*(1): pp.30.

Samiappan, S., Turnage, G., Hathcock, L., Casagrande, L. Stinson, P. and Moorhead, R., 2017. Using unmanned aerial vehicles for high-resolution remote sensing to map invasive *Phragmites australis* in coastal wetlands. *International Journal of Remote Sensing*, *38*(8-10): pp.2199-2217.

Sato, M., Ohsaki, H., Fukano, Y. and Yamawo, A. 2018. Self-discrimination in vine tendrils of different plant families. *Plant Signaling & Behavior*, doi: https://doi.org/10.1080%2F15592324.2018.1451710 .

Schmidt, K.S. and Skidmore, A.K. 2003. Spectral discrimination of vegetation types in a coastal wetland. *Remote Sensing of Environment*, *85*(1): pp.92-108.

Sellami, M.H., Albrizio, R., Čolović, M., Hamze, M., Cantore, V., Todorovic, M., Piscitelli, L. and Stellacci, A.M. 2022. Selection of hyperspectral vegetation indices for monitoring yield and physiological response in sweet maize under different water and nitrogen availability. *Agronomy*, *12*(2): p.489.

Selvaraj, S., Case, B.S. and White, W.L. 2021. Effects of location and season on seaweed spectral signatures. *Frontiers in Ecology and Evolution*, doi: https://doi.org/10.3389/fevo.2021.581852

Senturk, S., Sertel, E. and Kaya, S. 2013. Vineyards mapping using object based analysis. In *2013 Second International Conference on Agro-Geoinformatics (Agro-Geoinformatics)*, doi: http://dx.doi.org/10.1109/Argo-Geoinformatics.2013.6621881 .

Setyawan, D., Hanum, H., Achadi, T. and Paserena, K.D. 2023, April. The use of Drone for Identifying and Mapping of Revegetation Plant in Coal Post-mines in Tanjung Enim, South Sumatra, Indonesia. In *IOP Conference Series: Earth and Environmental Science*, doi: 10.1088/1755-1315/1162/1/012012 .

Shafri, H. Z. M., Anuar, M. I., Seman, I. A., & Noor, N. M. 2011. Spectral discrimination of healthy and *Ganoderma*-infected oil palms from hyperspectral data. *International Journal of Remote Sensing*, *32*(22), 7111–7129. Doi: https://doi.org/10.1080/01431161.2010.519003

Shahi, D. K. 2020. Vulnerability to Climate Change and Adaptation : A Case Study of Fresh Water Swamps and Wetlands of Doon Valley and Siwaliks. *Internat. J. Appl. Soc. Sci.,* available at: https://glslcities.org/wp-content/uploads/2015/09/Great_Lakes_Coastal_Wetland_Communities_-_Vulnerabilities_to_Climate_Change_and_Response_to_Adaptation_Strategies_2006_1.pdf . [Accessed on 24 January 2024].

Shahid, M., Khalid, S., Bibi, I., Bundschuh, J., Niazi, N.K. and Dumat, C. 2020. A critical review of mercury speciation, bioavailability, toxicity and detoxification in soil-plant environment: Ecotoxicology and health risk assessment. *Science of the Total Environment*, doi: https://doi.org/10.1016/j.scitotenv.2019.134749 .

Sharma, A., Kapoor, D., Wang, J., Shahzad, B., Kumar, V., Bali, A.S., Jasrotia, S., Zheng, B., Yuan, H. and Yan, D. 2020. Chromium bioaccumulation and its impacts on plants: an overview. *Plants*, doi: https://doi.org/10.3390%2Fplants9010100 .

Sharma, R., Vymazal, J. and Malaviya, P. 2021. Application of floating treatment wetlands for stormwater runoff: A critical review of the recent developments with emphasis on heavy metals and nutrient removal. *Science of The Total Environment*, doi: https://doi.org/10.1016/j.scitotenv.2021.146044 .

Shen, X., Dai, M., Yang, J., Sun, L., Tan, X., Peng, C., Ali, I. and Naz, I. 2022. A critical review on the phytoremediation of heavy metals from environment: Performance and challenges. *Chemosphere*, doi: https://doi.org/10.1016/j.chemosphere.2021.132979 .

Sheoran, A. S. 2006. Performance of three aquatic plant species in bench-scale acid mine drainage wetland test cells. *Mine Water and the Environment*, 25(1), 23-36.

Sileshi, A., Awoke, A., Beyene, A., Stiers, I., & Triest, L. 2020. Water purifying capacity of natural riverine wetlands in relation to their ecological quality. *Frontiers in Environmental Science*, doi: https://doi.org/10.3389/fenvs.2020.00039

Singh, P., Pandey, P.C., Petropoulos, G.P., Pavlides, A., Srivastava, P.K., Koutsias, N., Deng, K.A.K. and Bao, Y., 2020. Hyperspectral remote sensing in precision agriculture: Present status, challenges, and future trends. In *Hyperspectral remote sensing*. United Kingdom: Elsevier.

Sojka, M. and Jaskuła, J. 2022. Heavy metals in river sediments: contamination, toxicity, and source identification—a case study from Poland. *International Journal of Environmental Research and Public Health*, *doi: https://doi.org/10.3390/ijerph191710502*

Solom W. Newete. Barend, F.N. Erasmus, Isabel M. Weiersbye, Moses A. Cho & Marcus J. Byrne. 2014. Hyperspectral reflectance features of water hyacinth growing under feeding stresses of *Neochetina* spp. and different heavy metal pollutants. *International Journal of Remote Sensing*, 35:3: pp. 799-817.

Sridhar, B.M., Han, F.X., Diehl, S.V., Monts, D.L. and Su, Y. 2007. Spectral reflectance and leaf internal structure changes of barley plants due to phytoextraction of zinc and cadmium. *International journal of remote sensing*, *28*(5): pp.1041-1054.

Srivastava, D., Tiwari, M., Dutta, P., Singh, P., Chawda, K., Kumari, M. and Chakrabarty, D. 2021. Chromium stress in plants: toxicity, tolerance and phytoremediation. *Sustainability*, *13*(9): pp.4629.

Stamati, F.E., Chalkias, N., Moraetis, D. and Nikolaidis, N.P. 2010. Natural Attenuation of Nutrients in a Mediterranean Drainage Canal. *Journal of Environmental Monitoring*, *12*(1): pp.164-171.

Stern, B.R. 2010. Essentiality and toxicity in copper health risk assessment: overview, update and regulatory considerations. *Journal of Toxicology and Environmental Health, 73*(2-3): pp.114-127.

Stoltz, E. and Greger, M. 2002. Cottongrass effects on trace elements in submersed mine tailings. *Journal of Environmental Quality*, *31*(5): pp.1477-1483.

Sun, C.X., Li, C.C., Zhang, C.Y., Hao, L.Y., Song, M., Liu, W. and Zhang, Y.L. 2018. Reflectance and biochemical responses of maize plants to drought and re-watering cycles. *Annals of Applied Biology*, *172*(3): pp.332-345.

Sun, G., Wang, X., Sun, Y., Ding, Y. and Lu, W. 2019. Measurement method based on multispectral three-dimensional imaging for the chlorophyll contents of greenhouse tomato plants. *Sensors*, *19*(15): pp.3345.

Sun, Y., Wang, B. and Zhang, Z. 2023. Improving Leaf Area Index Estimation With Chlorophyll Insensitive Multispectral Red-Edge Vegetation Indices. *IEEE Journal of Selected Topics in Applied Earth Observations and Remote Sensing*, *16*: pp.3568-3582.

Sutton, G., Bownes, A., Visser, V., Mapaura, A. and Canavan, K. 2021. Progress and prospects for the biological control of invasive alien grasses Poaceae) in South Africa. *African Entomology*, *29*(3): pp.837-858.

Swayze, S., Rotondi, M., & Kuk, J. L. 2021. The associations between blood and urinary concentrations of metal metabolites, obesity, hypertension, type 2 diabetes, and dyslipidemia among us adults: nhanes 1999–2016. *Journal of Environmental and Public Health*, doi: https://doi.org/10.1155/2021/2358060

Sylvester, S.P., Soreng, R.J., Sylvester, M.D. and Clark, V.R. 2020. Festuca drakensbergensis (Poaceae): A common new species in the F. caprina complex from the Drakensberg Mountain Centre of Floristic Endemism, southern Africa, with key and notes on taxa in the complex including the overlooked F. exaristata. *PhytoKeys*, doi: https://doi.org/10.3897/phytokeys.162.55550 .

Taylor, S., Kumar, L., Reid, N. and Lewis, C.R. 2012. Optimal band selection from hyperspectral data for Lantana camara discrimination. *International Journal of Remote Sensing*, *33*(17), pp.5418-5437.

Tchounwou, P.B., Yedjou, C.G., Patlolla, A.K. and Sutton, D.J. 2012. Heavy metal toxicity and the environment. *Experientia supplementum , doi: https://doi.org/10.1007/978-3-7643-8340-4_6*

Terentev, A., Долженко, В., Fedotov, A., & Eremenko, D. 2022. Current state of hyperspectral remote sensing for early plant disease detection: a review. *Sensors*, 22(3), 757.

Tesfamichael, S.G., Newete, S.W., Adam, E. and Byrne, M.J. 2022. Discriminating pure Tamarix species and their putative hybrids using field spectrometer. *Geocarto International*, *37*(25), pp.7733-7752.

Thakur, A. and Kumar, A. 2024. Emerging paradigms into bioremediation approaches for nuclear contaminant removal: From challenge to solution. *Chemosphere*, *doi: https://doi.org/10.1016/j.chemosphere.2024.141369* .

Thoha, A.S., Putra, D.Y. and Muammar, A. 2023. September. Unmanned aerial vehicles (UAV) utilization for mapping the health of oil palm plants (Elaeis guineensis Jacq.). In *IOP Conference Series: Earth and Environmental Science*, doi: http://dx.doi.org/10.1088/1755-1315/1241/1/012072 .

Tognacchini, A., Rosenkranz, T., van der Ent, A., Machinet, G.E., Echevarria, G. and Puschenreiter, M. 2020. Nickel phytomining from industrial wastes: Growing nickel hyperaccumulator plants on galvanic sludges. *Journal of Environmental Management*, *doi: https://doi.org/10.1016/j.jenvman.2019.109798* .

Tondera, K., Shang, K., Vincent, G., Chazarenc, F., Hu, Y. and Brisson, J. 2020. Effect of plant species and nutrient loading rates in treatment wetlands for polluted river water under a subtropical climate. *Water, Air, & Soil Pollution*, *231*, pp.1-13.

Townsend, K., Lu, H., Sharley, D., & Pettigrove, V. 2019. Associations between microplastic pollution and land use in urban wetland sediments. *Environmental Science and Pollution Research*, 26(22), 22551-22561.

Tran, T.A. and Popova, L.P. 2013. Functions and toxicity of cadmium in plants: recent advances and future prospects. *Turkish Journal of Botany*, *37*(1), pp.1-13.

Tshapa, L., Naidoo, K. and Naidoo, G. 2021. Morphological and physiological responses of Arundo donax and Phragmites australis to waterlogging stress. *Flora*, doi: https://doi.org/10.1016/j.flora.2021.151816 .

US EPA. 2014. *Indicators: Wetland Vegetation (Plant Community) | US EPA*. Available at: https://www.epa.gov/national-aquatic-resource-surveys/indicators-wetland-vegetation-plant-community [Accessed 18 Mar. 2024].

US EPA. 2015. *Why are Wetlands Important? | US EPA*. Available at: https://www.epa.gov/wetlands/why-are-wetlands-important#:~:text=Some%20of%20these%20services%2C%20or,unique%20natural%20characteristics%20of%20wetlands. [Accessed 13 Feb. 2024].

Usgs.gov. 2024. *Spectral Library | U.S. Geological Survey*. Available at: https://www.usgs.gov/labs/spectroscopy-lab/science/spectral-library [Accessed 24 Mar. 2024].

Van Deventer, H. and Cho, M.A. 2014. Assessing leaf spectral properties of Phragmites australis impacted by acid mine drainage. *South African Journal of science*, *110*(7-8), pp.1-12.

Van Wilgen, B.W., Zengeya, T.A. and Richardson, D.M. 2022. A review of the impacts of biological invasions in South Africa. *Biological Invasions*, *24*(1), pp.27-50.

Verma, A. K. and Nandan, R. 2019. Knowledge based classifier based on backscattering coefficient for monitoring the crop growth analysis using multi-temporal images of space-borne synthetic aperture radar (sar) sensors. *The International Archives of the Photogrammetry, Remote Sensing and Spatial Information Sciences*, doi: https://doi.org/10.5194/isprs-archives-xlii-3-w6-643-2019

Vijayaragavan, M., Prabhahar, C., Sureshkumar, J., Natarajan, A., Vijayarengan, P. and Sharavanan, S. 2011. Toxic effect of cadmium on seed germination, growth and biochemical contents of cowpea (Vigna unguiculata L.) plants. *International Multidisciplinary Research Journal*, *1*(5): pp.1-3.

Vitt, P., Havens, K., Jolls, C.L. and Knight, T.M. 2020. Temporal variation in the roles of exotic and native plant species in plant–pollinator networks. *Ecosphere*, *doi:* https://doi.org/10.1002/ecs2.2981 .

Vivone, G. and Chanussot, J. 2020. Fusion of short-wave infrared and visible near-infrared WorldView-3 data. *Information Fusion*, *61*: pp.71-83.

Wahabzada, M., Mahlein, A.K., Bauckhage, C., Steiner, U., Oerke, E.C. and Kersting, K. 2016. Plant phenotyping using probabilistic topic models: uncovering the hyperspectral language of plants. *Scientific Reports*, doi: https://doi.org/10.1038/srep22482 .

Wang, S. and Shi, X. 2001. Molecular mechanisms of metal toxicity and carcinogenesis. *Molecular and Cellular Biochemistry*, *222*, pp.3-9.

Wang, X., Sun, Y., Li, S., & Wang, H. 2019. Spatial distribution and ecological risk assessment of heavy metals in soil from the raoyanghe wetland, china. Plos One, doi: https://doi.org/10.1371/journal.pone.0220409

Watanabe, T., Aedla, R., Hiraga, Y., & Sugimura, K. 2018. Development of geospatial model for preparing distribution of rare plant resources using uav/drone. *Indian Journal of Pharmaceutical Education and Research*, doi: https://doi.org/10.5530/ijper.52.4s.91

Watt, M. S., Buddenbaum, H., Leonardo, E. M. C., Estarija, H. J., Bown, H. E., Gómez-Gallego, M., & Zarco-Tejada, P. J. 2020. Using hyperspectral plant traits linked to photosynthetic efficiency to assess n and p partition. *ISPRS Journal of Photogrammetry and Remote Sensing*, 169: pp. 406-420.

Weiss, D.J., Mason, T.F., Zhao, F.J., Kirk, G.J.D., Coles, B.J. and Horstwood, M.S.A. 2005. Isotopic discrimination of zinc in higher plants. *New Phytologist*, *165*(3): pp.703-710.

Wen, W., Timmermans, J., Chen, Q., & Bodegom, P. 2020. A review of remote sensing challenges for food security with respect to salinity and drought threats. *Remote Sensing*, 13(1): pp. 6.

Wen, Y., Li, W., Yang, Z., Zhang, Q. and Ji, J. 2020. Enrichment and source identification of Cd and other heavy metals in soils with high geochemical background in the karst region, Southwestern China. *Chemosphere*, doi: https://doi.org/10.1016/j.chemosphere.2019.125620 .

Wibowo, Y. G., Wijaya, C., Halomoan, P., Yudhoyono, A., & Safri, M. 2022. Constructed wetlands for treatment of acid mine drainage: a review. *Jurnal Presipitasi : Media Komunikasi Dan Pengembangan Teknik Lingkungan*, 19(2): pp. 436-450.

Wójtowicz, A., Piekarczyk, J., Czernecki, B. and Ratajkiewicz, H. 2021. A random forest model for the classification of wheat and rye leaf rust symptoms based on pure spectra at leaf scale. *Journal of Photochemistry and Photobiology B: Biology*, doi: https://doi.org/10.1016/j.jphotobiol.2021.112278 .

World Health Organization. 2021. Mercury and human health: educational course. Available at: https://www.who.int/europe/publications/i/item/9789289055888 [Accessed 23 August 2023].

Wu, C., Liu, M., Liu, X., Wang, T. and Wang, L. 2019. Developing a new spectral index for detecting cadmium-induced stress in rice on a regional scale. *International Journal of Environmental Research and Public Health*, *16*(23): p.4811.

Xin, P., Wilson, A., Shen, C., Ge, Z., Moffett, K.B., Santos, I.R., Chen, X., Xu, X., Yau, Y.Y., Moore, W. and Li, L. 2022. Surface water and groundwater interactions in salt marshes and their impact on plant ecology and coastal biogeochemistry. *Reviews of Geophysics*, doi: https://doi.org/10.1029/2021RG000740 .

Xu, T., Weng, B., Yan, D., Wang, K., Li, X., Bi, W., Li, M., Cheng, X. and Liu, Y. 2019. Wetlands of international importance: Status, threats, and future protection. *International Journal of Environmental Research and Public Health*, *16*(10): pp.1818.

Yan, A., Wang, Y., Tan, S.N., Mohd Yusof, M.L., Ghosh, S. and Chen, Z. 2020. Phytoremediation: a promising approach for revegetation of heavy metal-polluted land. *Frontiers in Plant Science*, *11*: pp.359.

Yang, L., Zhang, Y., Wang, F., Luo, Z., Guo, S. and Strähle, U. 2020. Toxicity of mercury: Molecular evidence. *Chemosphere*, doi: https://doi.org/10.1016/j.chemosphere.2019.125586 .

Yang, W. and Zhai, R. 2022. What can aerial phenotyping do and bring to us (breeders)? *The New Phytologist*, *236*(4): pp.1229.

Yang, Y. and Shen, Q. 2020. Phytoremediation of cadmium-contaminated wetland soil with Typha latifolia L. and the underlying mechanisms involved in the heavy-metal uptake and removal. *Environmental Science and Pollution Research*, *27*(5): pp.4905-4916.

Ye, Z.H., Whiting, S.N., Lin, Z.Q., Lytle, C.M., Qian, J.H. and Terry, N. 2001. Removal and distribution of iron, manganese, cobalt, and nickel within a Pennsylvania constructed wetland treating coal combustion by-product leachate. *Journal of Environmental Quality*, 30(4): pp.1464-1473.

Yendrek, C. R., Tomaz, T., Montes, C. M., Cao, Y., Morse, A. M., Brown, P. J., … & Ainsworth, E. A. 2016. High-throughput phenotyping of maize leaf physiological and biochemical traits using hyperspectral reflectance. *Plant Physiology*, 173(1): 614-626. https://doi.org/10.1104/pp.16.01447

Yu, Li, Shi Kaiyi, Jie Yuan, and Kuang Qiyu. 2021. “Evaluation of heavy metal pollutants from plateau mines in wetland surface deposits”, *Frontiers in Environmental Science*, doi: https://doi.org/10.3389/fenvs.2020.557302

Yusuf, M., Fariduddin, Q., Hayat, S., & Ahmad, A. 2010. Nickel: an overview of uptake, essentiality and toxicity in plants. *Bulletin of Environmental Contamination and Toxicology*, 86(1): pp. 1-17.

Zakariah, M. 2014. Classification of large datasets using Random Forest Algorithm in various applications: Survey. *International Journal of Engineering and Innovative Technology (IJJEIT)*, *4*(3). Available at: https://faculty.ksu.edu.sa/sites/default/files/classification_of_large_datasets_using_random.pdf

Zamora-Ledezma, C., Negrete-Bolagay, D., Figueroa, F., Zamora-Ledezma, E., Ni, M., Alexis, F. and Guerrero, V.H., 2021. Heavy metal water pollution: A fresh look about hazards, novel and conventional remediation methods. *Environmental Technology & Innovation*, doi: https://doi.org/10.1016/j.eti.2021.101504

Zarco-Tejada PJ, Hornero A, Hernández-Clemente R, Beck PSA. 2018. Understanding the temporal dimension of the red-edge spectral region for forest decline detection using high-resolution hyperspectral and Sentinel-2a imagery. *ISPRS J Photogramm Remote Sens*, doi: 10.1016/j.isprsjprs.2018.01.017.

Zaynab, M., Al-Yahyai, R., Ameen, A., Sharif, Y., Ali, L., Fatima, M., Khan, K.A. and Li, S. 2022. Health and environmental effects of heavy metals. *Journal of King Saud University-Science*, doi: https://doi.org/10.1016/j.jksus.2021.101653 .

Zellweger, F., De Frenne, P., Lenoir, J., Rocchini, D. and Coomes, D. 2019. Advances in microclimate ecology arising from remote sensing. *Trends in Ecology & Evolution*, *34*(4): pp.327-341.

Zhai, Y., Zhou, L., Qi, H., Gao, P. and Zhang, C. 2023. Application of Visible/Near-Infrared Spectroscopy and Hyperspectral Imaging with Machine Learning for High-Throughput Plant Heavy Metal Stress Phenotyping: A Review. *Plant Phenomics*, doi: https://doi.org/10.34133%2Fplantphenomics.0124 .

Zhang, C., Ren, H., Liang, Y., Liu, S., Qin, Q. and Ersoy, O.K. 2017. Advancing the PROSPECT-5 model to simulate the spectral reflectance of copper-stressed leaves. *Remote Sensing*, *9*(11): pp.1191.

Zhang, D., Jiang, Q., Liang, D., Huang, S. and Liao, J. 2021. The potential application of giant reed (Arundo donax) in ecological remediation. *Frontiers in Environmental Science*, doi: https://doi.org/10.3389/fenvs.2021.652367 .

Zhang, N., Zhao, X., Liu, T., Lei, M., Wang, C. and Wang, Y. 2019. Layout planning of highway transportation environment monitoring network: The case of Xinjiang, China. *Sustainability*, *12*(1): pp.290.

Zhao, X., Zhang, J., Huang, Y., Tian, Y. and Yuan, L. 2022. Detection and discrimination of disease and insect stress of tea plants using hyperspectral imaging combined with wavelet analysis. *Computers and Electronics in Agriculture*, doi: https://doi.org/10.1016/j.compag.2022.106717 .

Zhao, Y., Mao, D., Zhang, D., Wang, Z., Du, B., Yan, H., Qiu, Z., Feng, K., Wang, J. and Jia, M., 2022. Mapping phragmites Australis aboveground biomass in the momoge wetland ramsar site based on Sentinel-1/2 images. *Remote Sensing*, *14*(3): pp.694.

Zheng, G. and Moskal, L. M. (2009). Retrieving leaf area index (lai) using remote sensing: theories, methods and sensors. *Sensors*, 9(4): 2719-2745.

Zhou, C., Chen, S., Zhang, Y., Zhao, J., Song, D. and Liu, D. 2018. Evaluating metal effects on the reflectance spectra of plant leaves during different seasons in post-mining areas, China. *Remote Sensing*, doi: https://doi.org/10.3390/rs10081211 .

Zhu, L., Zhao, X., Lai, L., Wang, J., Jiang, L., Ding, J., Liu, N., Yu, Y., Li, J., Xiao, N. and Zheng, Y. 2013. Soil TPH concentration estimation using vegetation indices in an oil polluted area of eastern China. *PloS one*, doi: https://doi.org/10.1371/journal.pone.0054028